Am J Transl Res 2023;15(1):27-46
www.ajtr.org /ISSN:1943-8141/AJTR0144732

Original Article

PTTG1IP (PBF) is a prognostic marker and correlates with immune infiltrate in ovarian cancer

Ruiqiong Ma, Zhijian Tang, Jianliu Wang

Department of Obstetrics and Gynecology, Peking University People's Hospital, Beijing 100044, China

Received June 13, 2022; Accepted November 8, 2022; Epub January 15, 2023; Published January 30, 2023

Abstract: Objective: An oncogenic protein, pituitary tumor transforming gene 1 binding factor (PTTG1IP, also called PBF), has been found to be expressed in various cancers. However, few studies have explored its prognostic significance and biologic function in epithelial ovarian cancer (EOC). Methods: Based on the Cancer Genome Atlas (TCGA) database, this study determined the differential expression of PBF at the mRNA level in EOC and normal tissues, which was then verified using real-time PCR and western blotting. Moreover, the Kaplan-Meier method and the Cox regression method were adopted to assess the clinical value of PBF in EOC. A nomogram model was constructed to evaluate the prognostic performance of PBF in EOC. Gene set enrichment analysis (GSEA) was employed to evaluate the signaling and pathway enrichment of PBF in EOC. The association between PBF expression and tumor-infiltrating immune cells (TIICs) in EOC was examined by single-sample GSEA and TIMER. Results: PBF was significantly higher in EOC than normal tissues as shown through TCGA database, and this result was verified by qRT-PCR and western blotting of EOC tissues and different cell lines. High PBF was associated with tumor size and lymphatic metastasis status. Kaplan-Meier (KM) analysis indicated that high PBF expression correlated with poor prognosis in patients with EOC ($P < 0.0001$). Moreover, multivariate Cox regression analysis was used to verify that PBF is an independent prognostic factor for EOC. The nomogram model exhibited moderate predictive accuracy and clinical utility in predicting EOC prognosis. The GSEA revealed that the expression of signaling pathways, such DNA damage replication, p53 pathway, Akt phosphorylation pathway, and estrogen-dependent nuclear pathway, were increased in the phenotype with high PBF expression. PBF expression was associated with neutrophil cells, iDC cells, NK cells, and Tem cells. Conclusion: As a prognostic biomarker for EOC, PBF was found to be correlated with immune infiltration, and may therefore be a promising target for immunotherapy for EOC.

Keywords: EOC, biomarkers, PTTG1IP, prognosis, immune infiltration

Introduction

Epithelial ovarian cancer (EOC) ranks among the global top five common causes of female cancer-related death and is one of the most malignant gynecological cancers [1]. Due to a lack of feasible methods for early detection, most cases are diagnosed during the advanced stage (FIGO stage III/IV disease) [2]. Consequently, the 5-year overall survival (OS) rate of ovarian cancer is below 50% (FIGO stage III/IV disease, 5-year OS rate of 29%) [3, 4]. Standard therapy is composed of cytoreductive surgery accompanied by platinum and taxane-based chemotherapy. Though the initial response rates of patients after surgery and first-line chemotherapy can reach over 80%, most of these patients eventually experience recurrence due to rapid progression and chemoresistance [5]. Several targeted treatment methods, such as vascular endothelial growth factor (VEGF) inhibitors, have been incorporated into clinical settings as first-line or second-line therapy methods for recurrent disease [6]. However, due to resistance against PARP inhibitors, a majority of patients are likely to develop recurrence due to cancer progression [7]. Therefore, it is critical to explore novel diagnostic or prognostic biomarkers and therapeutic targets for EOC.

pituitary tumor transforming gene 1 binding factor (PTTG1IP, also called c21orf3, PTTG1-

binding factor, or PBF) is a widely expressed proto-oncogene, which was initially measured to be a 22 kDa protein involved in binding to [8]. Previous research has demonstrated that PBF is extensively expressed in normal tissues, such as the thyroid gland, and placenta [9]. Increasing evidence suggests that PBF expression is elevated in different cancers, such as thyroid, breast, and colorectal cancers [10-12]. In addition, PBF overexpression is significantly related to a poor outcome in many cancers. Compared to normal thyroid tissues, PBF is a novel transformation-related and oncogenic gene that is overexpressed in thyroid cancer, and high levels of PBF expression are correlated with neoplasm recurrence and shorter disease-specific survival [13]. Though PBF has hardly been identified in normal breast tissues, it is highly expressed in epithelial cells of ERα-positive breast tumors. Moreover, PBF upregulation in breast MCF-7 cells significantly increases cell invasion *in vitro*. These results further support the fact that PBF modulates the estrogen-mediated invasion of breast cancer cells by acting as a proto-oncogene [10, 14]. Similarly, PBF is also upregulated in colorectal cancer and serves as a novel adjuster through the inhibition of p53 activity, especially in invasive wild-type p53 and mutant p53 tumors, indicating that PBF may be a novel prognostic biomarker of colorectal cancer. However, PBF is apparently downregulated at the mRNA level in NSCLC tissues compared to adjacent tissues. Moreover, the upregulation of PBF significantly inhibits cell proliferation [15]. In summary, the above findings confirm that PBF expression is correlated with endocrine activity and tumorigenesis. However, the role of PBF in EOC has not been elucidated.

Therefore, we analyzed PBF expression in EOC and its association with clinicopathologic features and prognosis, based on data obtained from TCGA. Additionally, a nomogram combined with PBF expression and clinical clinicopathological features was constructed to forecast the risk of peritoneal metastasis for EOC patients. GSEA was applied to evaluate possible molecular functions of PBF. Subsequently, ssGSEA and TIMER were also performed to verify the relationship between PBF expression and TIICs in EOC. This study proves that high expression of PBF is associated with the unsatisfactory OS of EOC patients and that pathways involved in DNA damage replication, Toll pathway, extracellular matrix interaction, p53 pathway, B cell receptor complexes, Wnt signaling pathway, Akt phosphorylation pathway, estrogen-dependent nuclear pathway, and the FGF pathway are associated with PBF expression. Furthermore, we found a correlation between PBF and levels of TIICs, especially in neutrophil cells, iDC cells, NK cells, and Tem cells. Thus, PBF can function as a novel predictive biomarker and immunotherapy target for EOC patients.

Materials and methods

Data collection

The RNA-seq data from TCGA and Genotype-Tissue Expression (GTEx) databases, including data on normal and 33 types of cancer tissue samples were collected from sets of the University of California Santa Cruz (UCSC) Xena browser platform (https://xenabrowser.net/). The gene expression and clinicopathologic data were downloaded for further bioinformatics analysis. According to the intermediate value of PBF expression used as the cutoff, all EOC patients were categorized into low-expression and high-expression groups. The GSE40595 dataset of EOC was collected from the Gene Expression Omnibus (https://www.ncbi.nlm.nih.gov/geo/) database using the GEO query R package and was used for validation. Since data were collected from TCGA and GEO databases, approval from the ethics committee was not required for this study.

Human protein atlas (HPA)

HPA (https://www.proteinatlas.org/), a network database, provides immunohistochemistry (IHC) data generated from normal and cancer tissue profiles. The protein expression of PBF in normal tissues and in EOC tissues was measured using IHC data from the HPA database.

Tissue specimens, and cell lines, and culture

We collected 30 ovarian cancer tissues from patients who had undergone surgery at Peking University People's Hospital between January 2019 and January 2020. As a control, we also acquired 5 normal ovarian samples from bilateral salpingo-oophenrectomy cases. The diag-

nosis of ovarian cancer grade was performed by two experienced pathologists. All patients involved provided written informed consent, and this study was approved by the Ethics Commitee of the Peking University People's Hospital. Clinical tissues from EOC patients were used to detect expression at the mRNA and protein level.

Five ovarian cancer cell lines (SKOV3.ip, SKOV3, CAOV3, OVCAR3, and ES2) were also collected for this study. CAOV3 was sustained in DMEM supplemented with 10% FBS; the SKOV3.ip cells, OVCAR3 cells, and ES2 cells were sustained in RPMI-1640 supplemented with 10% FBS; while SKOV3 cells were grown in McCoy's 5A supplemented with 10% FBS. The cells were all cultured at 37°C in a humid incubator with 5% CO_2. Total RNA and protein were acquired from the ovarian cancer cell line specimens.

RNA isolation and qRT-PCR

The RNA was extracted from the EOC samples and EOC cell lines by TRIzol reagent (Invitrogen, USA). RNA reverse transcription was achieved through the PrimeScript™ RT reagent Kit (Takara), which was measured by quantitative PCR using the SYBR Green PCR Kit (Applied Biosystems, USA) based on the manufacturer's instructions. The forward primer of the reference gene was AAGGTGAAGGTCGGAGTCAAC, and the reverse primer of the reference gene was GGGGTCATTGATGGCAACAATA. The forward primer of the target gene was CCTGTGAAGAGTGCCTGAAGAACG, and the reverse primer of the target gene was GAAGCGTCGGGACTGATGTGC. The $2^{-\Delta\Delta CT}$ approach was adopted to analyze the results, and the gene expression was normalized relative to GAPDH.

Western blotting analysis

The total proteins extracted from the EOC tissues and EOC cell lines were lysed using the RIPA cell lysate (CST, USA), and were further separated using SDS-PAGE and then transferred to a polyvinylidene fluoride (PVDF) membrane. After blocking using TBS-T with 5% milk for one hour at room temperature, the membranes were cultured with the primary antibodies against PTTG1IP (1:1000, Abcam, USA) at 4°C overnight and with the secondary antibody (1:3000, Abcam, USA). The relative levels of the target proteins were consistent with the protein band intensity of the grey value of the internal reference band (GAPDH). The whole experimental process was performed in triplicate.

Analysis of the differentially expressed genes (DEGs) between the low-PBF and high-PBF expression groups of EOC patients

Using the RNA-seq data based on low-PBF and high-PBF expression groups in the EOC samples, differential mRNA expression was analyzed via the "DESeq2" R package. DEGs with $|\log_2 FC| > 1.5$ and false discovery rate (FDR) < 0.05 were incorporated into the following analyses, while volcano plots and heat maps were created using the ggplot2 package in R.

Analysis of gene ontology (GO) and pathway enrichment

GO and Kyoto Encyclopedia of Genes and Genomes (KEGG) enrichment analysis of the PBF-related DEGs were conducted using the cluster Profiler package. GO was utilized to identify the corresponding biologic processes (BP), cell components (CC), and molecular functions (MF). A *P*-value of < 0.05 was set as the cut-off criterion for the Benjamini and Hochberg (BH) method.

GSEA and protein-protein interaction (PPI) network

GSEA was employed to verify a significant increase in gene sets between low-PBF and high-PBF expression groups. Pathways with a FDR < 0.25 and a nominal $P < 0.05$ were regarded as significantly enriched pathways. The PPI network of PBF was evaluated using the Search Tool for the Retrieval of Interacting Genes (STRING) database (https://string-db.org/) with a minimum interaction score of 0.7.

Immune infiltration analysis using single-sample GSEA and tumor immune cells to assess resource (TIMER)

The immune-cell infiltration levels of EOC in the TCGA cohorts were estimated using the single-sample GSEA method in the GSVA R package. In total, 24 different types of immune cells, such as dendritic cells (DCs), T helper 17 (Th17) cells, eosinophils, neutrophils, regulato-

ry T cells, activated DCs, B cells, $CD8^+$ T cells, T helper cells, and effector memory T cells, could be discriminated in this study. The immune responses of the 24 TIICs were measured to assess their correlation with PBF expression in the EOC. The correlation analysis between immune infiltration and PBF expression in EOC was done using the Spearman's rank-correlation coefficient. The Wilcoxon rank sum test was used to compare the infiltration of immune cells between the low-PBF and high-PBF expression groups. $P < 0.05$ was used to indicate statistical significance.

Tumor immune to assess resource (TIMER, https://cistrome. shinyapps.io/timer/) is a trustworthy database that can be used to comprehensively evaluate the TIICs identified among the many different cancer types included in TCGA. The Kaplan-Meier method was applied to measure the prognostic value of PTTG1IP in 6 different types of immune cells: B cells, $CD8^+$ T cells, dendritic cells (DC), $CD4^+$ T cells, neutrophils, and macrophages. TIMER was adopted to explore the association between PBF and immune cell markers to assess the effect of PBF on tumor immunity. The immune cells included monocytes, $CD8^+$ T cells, neutrophils, B cells, M1 macrophages, M2 macrophages, T helper 1 (Th1) cells, T helper 2 (Th2) cells, natural killer (NK) cells, DCs, and exhausted T cells.

Statistical analysis and nomogram

The comparison of PBF expression between different clinicopathologic groups was performed using the Kruskal-Wallis test, Wilcoxon signed test, and the Wilcoxon rank sum test. Additionally, the receiver operating characteristic (ROC) curve was used to distinguish EOC from normal tissue. The associations between PBF expression and clinicopathologic features were measured through logistic regression. Survival analyses for disease-specific survival (DSS) and OS were conducted using both the Kaplan-Meier method and Cox regression analysis. The independent prognostic value of PBF was assessed using univariate and multivariate Cox regression models by R (Version v.3.6.2). A two-tailed *P*-value of < 0.05 was considered significant.

A nomogram was built based on the factors that were of significance to multivariate prognostic parameters and clinicopathologic characteristics using the rms R package (version 5.1.2, https://cran.r-project.org/web/packages/rms/). The nomogram could assess the DSS and 1, 3, and 5-year OS in EOC patients. Discriminations between observations and predictions were quantitatively assessed using the concordance index (C-index). Calibration plots were generated by comparing the relationships between the nomogram prediction probability and the observations. A *P*-value of < 0.05 was considered significant.

Results

PBF was upregulated in EOC

We first evaluated PBF expression in the TCGA and GTEx pan-cancer database, and observed higher PBF expression in a majority of tumors, including breast invasive carcinoma (BRCA), cholangiocarcinoma (CHOL), thyroid carcinoma (THCA), skin melanoma (SKCM), uterine sarcoma (UCS), and endometrial cancer (UCEC) (**Figure 1A**). In particular, higher PBF expression was observed in EOC from the TCGA cohort and GSE40595 cohort than in normal tissues ($P < 0.001$, **Figure 1B** and **1C**). Moreover, the diagnostic value of PBF in EOC patients was assessed by ROC curve analysis. The area under the curve (AUC) of the ROC curve of PBF was 0.606 (95% confidence interval [CI] = 0.556-0.657) (**Figure 1D**), indicating that PBF can be used to effectively discriminate EOC tissues from normal tissues.

The immunohistochemistry staining results of HPA suggested that PBF was strongly expressed in EOC tissues but rarely expressed in normal tissues (**Figure 2A**). Additionally, the mRNA and protein expression patterns of PBF in EOC tissues obtained from Peking University *People's Hospital (PKUPH)* and the EOC cell lines were explored. We observed that the mRNA and protein expression of PBF were higher in EOC tissues than in normal tissues ($P = 0.004$ and $P = 0.007$) (**Figure 2B**). Among all the EOC cell lines, a relatively higher level of PBF expression at mRNA and protein levels was observed in SKOV3.ip, SKOV3 and ES2 cells, and a lower level was found in CAOV3 cells and OVCAR3 cells (**Figure 2C**). In summary, these results suggest that PBF may affect the pathogenesis of EOC.

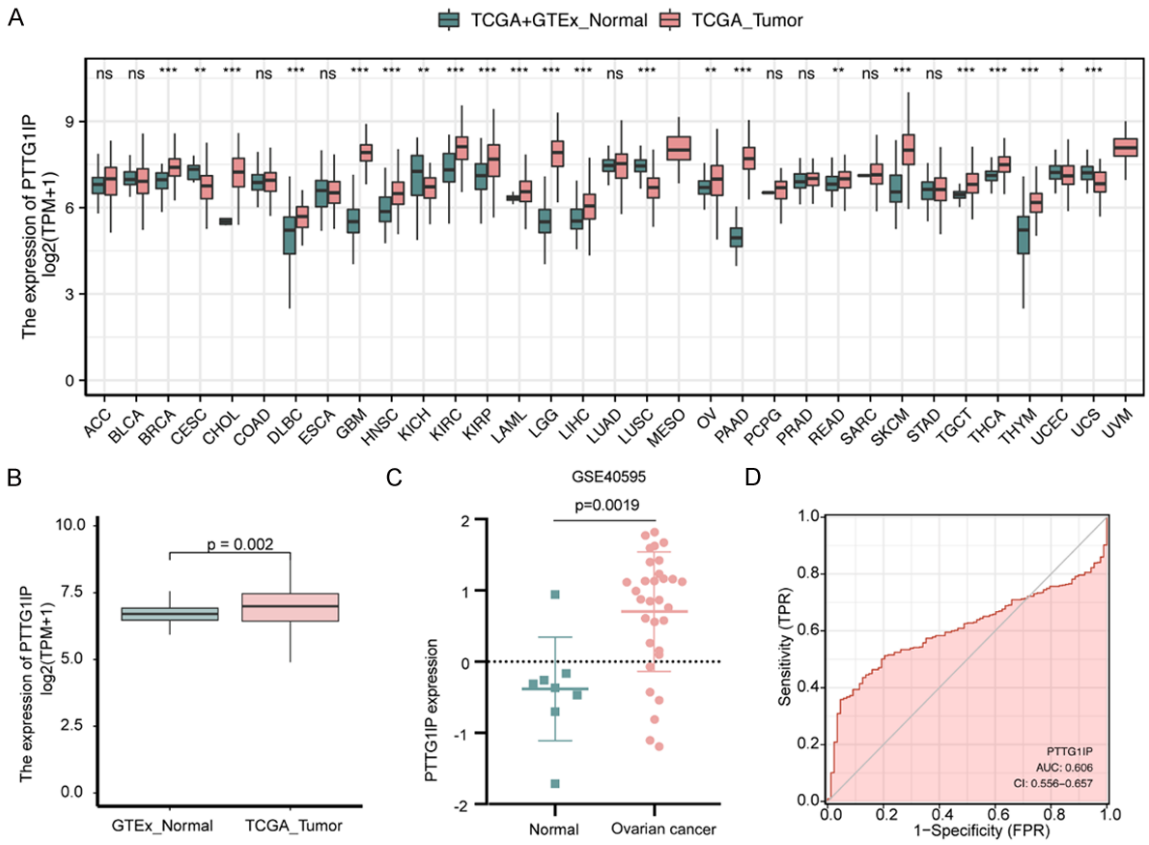

Figure 1. PBF expression in patients with EOC. A. PBF expression levels in various types of tumor obtained from TCGA database; B. Expression levels of PBF in EOC and normal tissues in TCGA database; C. The PBF expression in EOC and normal tissues in the GEO database; D. ROC analysis of PBF in EOC. PBF, PTTG1-binding factor; EOC, epithelial ovarian cancer.

Connection between PBF expression and the clinicopathologic characteristics of EOC

To examine the connection between PBF expression and the clinicopathologic features of EOC patients, PBF expression data and clinical data on EOC samples were extracted from the TCGA database (Supplementary Table 1) and analyzed. As **Table 1** shows, PBF expression was highly associated with primary treatment outcome (P = 0.028), residual tumors (P = 0.021), and age (P = 0.012). Nevertheless, PBF expression was not strongly associated with other measures, including International Federation Organization of Gynecology and Obstetrics (FIGO) stage, histological grade, anatomical neoplasm subdivision, venous invasion, lymphatic invasion, and TP53 status (all P > 0.05). Furthermore, the univariate logistic regression results confirmed that PBF expression was also highly associated with clinical characteristics, such as primary treatment outcome (CR vs. PD&SD&PR) (OR = 0.60 (0.36-0.98), P = 0.043) and residual tumors (RD vs. NRD) (1.99 (1.15-3.51), P = 0.015), but not FIGO stage, histologic grade, anatomic neoplasm subdivision, venous invasion, lymphatic invasion, and TP53 status (Supplementary Table 2). The analysis results verified that EOC patients with high PBD expression had more progression of EOC.

PBF is an independent prognostic predictor of EOC

To measure the prognostic value of PBF in EOC patients, we used EOC sample data obtained from TCGA databases. It was observed that high PTTG1IP expression was strongly associated with a worse OS (HR = 1.42 (1.09-1.85), P = 0.009) and DSS (HR = 1.49 (1.13-1.98), P = 0.005) (**Figure 3A** and **3B**). Moreover, univari-

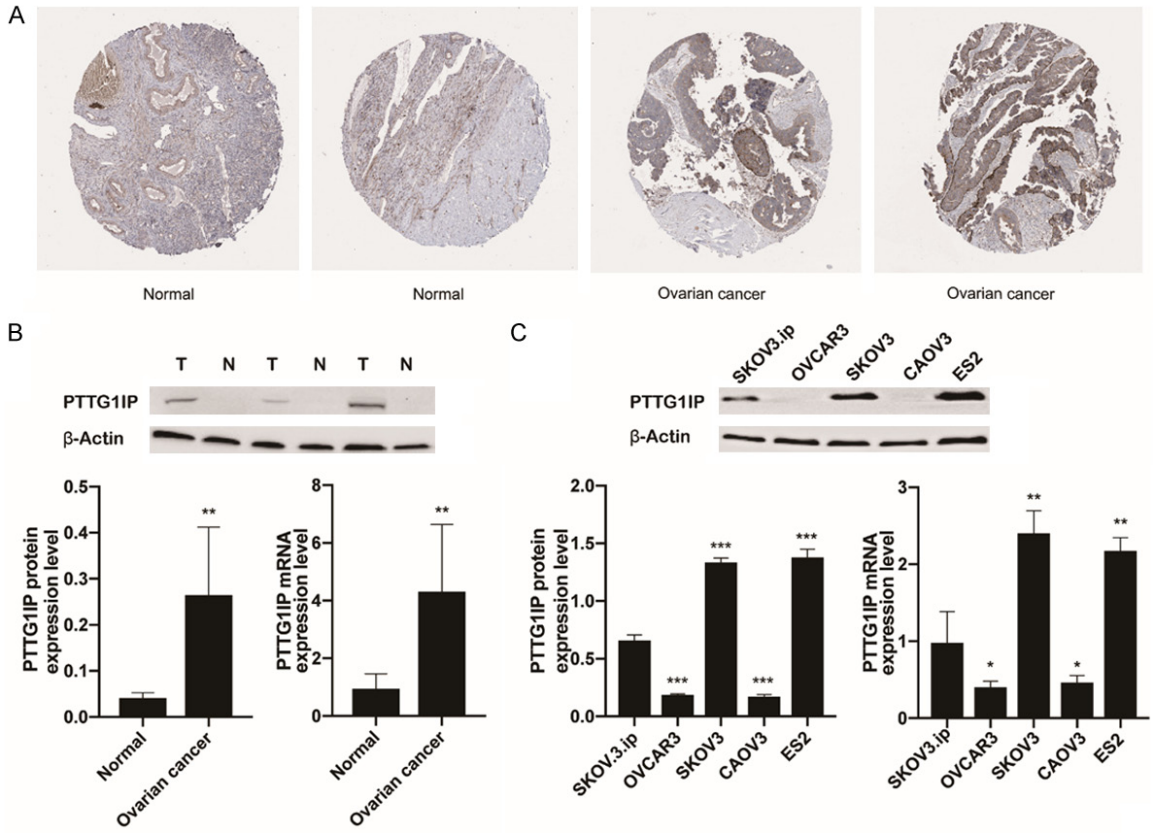

Figure 2. PBF expression in EOC tissues and cell lines. A. Representative IHC staining patterns of PBF in EOC tissues obtained from the HPA database; B. PBF protein and mRNA expression in normal tissues (n = 5) and EOC tissues (n = 30); C. PBF protein and mRNA expression in five EOC cell lines (SKOV3.ip, OVCAR3, SKOV3, CAOV3, and ES2). PBF, PTTG1-binding factor; EOC, epithelial ovarian cancer.

ate analysis showed that primary thermal outcome, residual tumors, and PBF expression were associated with DSS, while primary thermal outcome, residual tumors, age, and PBF expression were associated with OS (**Table 2**). As shown in **Table 2**, the multivariate analysis was performed by adjusting variables with $P < 0.1$ in the univariate analysis. Primary therapy outcome and high PBF expression were independent predictors for OS as given in the multivariate analyses ($P < 0.05$). Accordingly, primary treatment outcome, residual tumors, and age were independent prognostic values for DSS ($P < 0.05$). Hence, the results confirmed that high PBF expression is an independent predictor associated with adverse prognosis of EOC patients.

A subgroup analysis was conducted to measure the effect of *PBF* expression on OS and DSS and the analysis confirmed that the predictive effect of *PBF* expression in EOC was significant for OS in Stage III and G3 patients ($P < 0.05$) (**Figure 3C** and **3D**). This effect was also significant for DSS in Stage III and G3 patients ($P < 0.05$) (**Figure 3E** and **3F**). The multivariate Cox regression analysis also demonstrated that *PBF* was the only prognostic indicator of both DSS and OS at Stage III and G3 of EOC patients (Supplementary Tables 3 and 4). The above data indicated that a high *PBF* level was associated with a poor prognosis.

Construction and validation of a PBF based nomogram

A nomogram that integrated PBF expression with other clinical elements (primary treatment outcome, tumor residual, and age) was constructed to predict the 1, 3, and 5 year DSS and OS of patients with EOC. The total number of points on the nomogram manifested a poorer prognosis. The C-index for OS and DSS prediction were 0.685 (0.663-0.708) and 0.694

Table 1. Clinical characteristics of ovarian cancer patients based on TCGA

Feature	Level	Low expression of PTTG1IP	High expression of PTTG1IP	p	test
n		188	188		
FIGO stage (%)	Stage I	1 (0.5%)	0 (0.0%)	0.321	exact
	Stage II	13 (7.0%)	9 (4.8%)		
	Stage III	149 (79.7%)	144 (77.4%)		
	Stage IV	24 (12.8%)	33 (17.7%)		
Histologic grade (%)	G1	0 (0.0%)	1 (0.5%)	0.166	exact
	G2	17 (9.3%)	25 (13.7%)		
	G3	166 (90.7%)	156 (85.2%)		
	G4	0 (0.0%)	1 (0.5%)		
Primary therapy outcome (%)	CR	115 (75.2%)	98 (64.5%)	0.028	
	PD	12 (7.8%)	15 (9.9%)		
	PR	13 (8.5%)	30 (19.7%)		
	SD	13 (8.5%)	9 (5.9%)		
Anatomic neoplasm subdivision (%)	Bilateral	119 (67.6%)	134 (75.3%)	0.139	
	Unilateral	57 (32.4%)	44 (24.7%)		
Venous invasion (%)	No	21 (41.2%)	19 (36.5%)	0.779	
	Yes	30 (58.8%)	33 (63.5%)		
Tumor residual (%)	NRD	42 (25.1%)	24 (14.5%)	0.021	
	RD	125 (74.9%)	142 (85.5%)		
Lymphatic invasion (%)	No	24 (32.0%)	24 (32.9%)	1.000	
	Yes	51 (68.0%)	49 (67.1%)		
TP53 status (%)	Mut	128 (90.8%)	120 (90.2%)	1.000	
	WT	13 (9.2%)	13 (9.8%)		
Age (%)	≤ 60	95 (50.5%)	112 (59.6%)	0.097	
	> 60	93 (49.5%)	76 (40.4%)		
Age (median [IQR])		60.00 [52.00, 70.00]	57.00 [49.00, 66.00]	0.012	nonnorm

Abbreviations: FIGO, International Federation of Gynecology and Obstetrics.

(0.670-0.717) (**Figure 4A** and **4B**), respectively. Furthermore, the calibration curves suggested that the predicted rates matched the actual survival rates at 1-, 3-, and 5 years (**Figure 4C** and **4D**). These results confirmed that the nomogram showed a moderate degree of accuracy in predicting the OS of EOC patients.

Identifying the DEGs

The DESeq2 package was adopted to detect DEGs between the high-PBF and low-PBF groups. The criteria of the DEGs were modified to a p value < 0.05 and $|\log_2(\text{fold change})| > 1$. A total of 278 DEGs (11 upregulated and 267 downregulated genes) were identified (**Figure 5A**). The expression values of the top ten DEGs between the high-PBF and low-PBF groups are shown in **Figure 5B**. The adjusted P value and $\log_2$FC of each DEG are shown in Supplementary Table 5.

Potential mechanism by which PBF regulates BRC progression

To elucidate the biological functions of PBF in EOC and illustrate key signaling mechanisms regulated by PBF, we performed GO functional enrichment analysis and KEGG pathway analysis. Subsequently, the GO analysis results of the DEGs were classified into three main functional groups: cellular components (GO-CC), biologic processes (GO-BP), and molecular functions (GO-MF) (Supplementary Table 6). The BP enrichment indicated that genes were predominantly involved in mRNA 5'-splice site recognition, mRNA splice site selection, antimi-

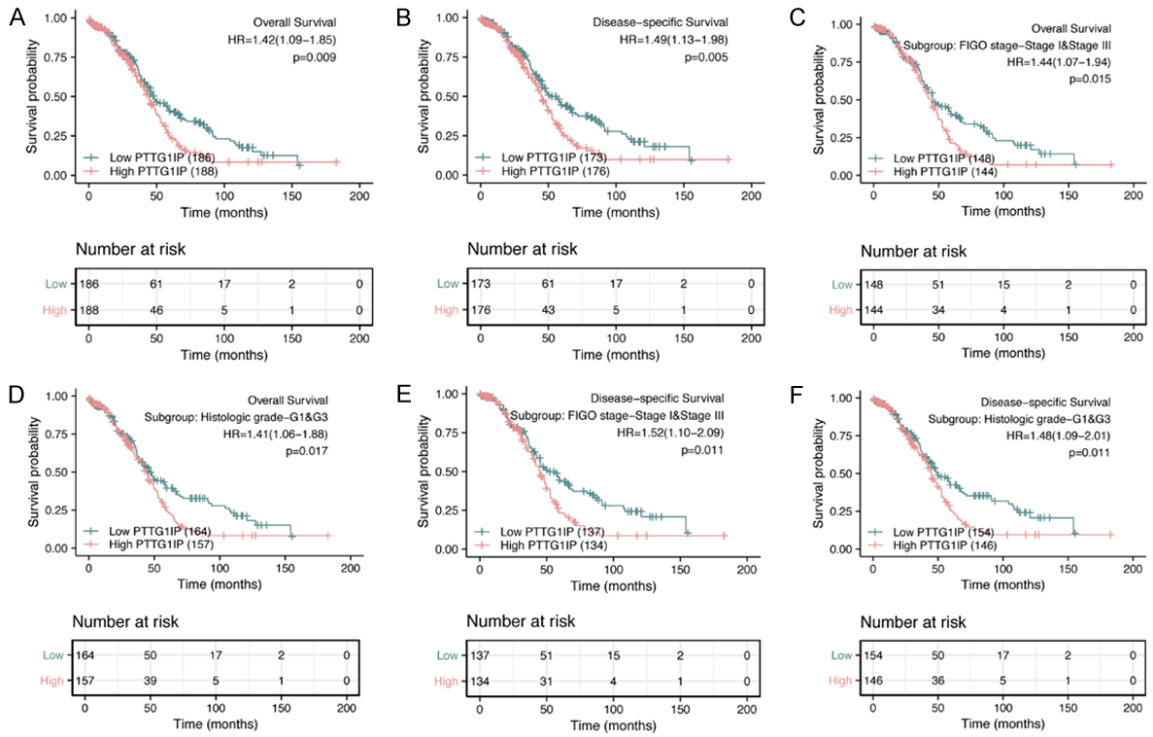

Figure 3. Prognostic value of PBF expression in EOC. A. Survival curves of OS constructed using TCGA data; B. Survival curves of DSS constructed using TCGA data; C. OS survival curves of stages I and III subgroups between PBF-high and -low expression EOC cases; D. OS survival curves of stages G1 and 3 subgroups between PBF-high and -low expression EOC cases; E. DSS survival curves of I and III subgroups between PBF-high and -low EOC cases; F. DSS survival curves of G1 and 3 subgroups between PBF-high and -low EOC cases. PBF, PTTG1-binding factor; EOC, epithelial ovarian cancer; OS, overall survival; DSS, disease specific survival.

crobial humoral response, nucleosome positioning, and spliceosomal complex assembly. Also, genes from the CC terms were significantly associated with spliceosomal snRNP complex, collagen-containing extracellular matrix, and protein-DNA complex. MF analysis also revealed a positive correlated with hormone activity, endopeptidase inhibitor activity, and receptor ligand activity (**Figure 5C-E**). The KEGG analysis results showed that the genes were highly upregulated in protein digestion and absorption, neuroactive ligand-receptor interaction, RNA transport, and spliceosomes (**Figure 5F**). The findings of both analyses confirmed that high PBF expression was associated with multiple biological signaling pathways in EOC.

GSEA identified a PBF-related signaling pathway

To further identify the effects of PBF on EOC, we conducted a GSEA analysis on RNA-seq data on EOC patients from TCGA database. Based on the PBF expression levels in TCGA dataset, EOC samples were sorted into low-PBF and high-PBF expression groups. The significantly enriched biological pathways are shown in **Figure 6**, and include DNA damage replication, Toll pathway, extracellular matrix interaction, P53 pathway, B cell receptor complexes, Wnt signaling pathway, Akt phosphorylates pathway, estrogen-dependent nuclear pathway and FGF pathway, which reveals possible regulatory mechanisms of PBF in EOC.

PPI

To detect the role of PBF in EOC, we established a PPI network using the STRING database and evaluated the relationships between the related genes (**Figure 7**).

The connection between PBF expression and immune infiltration

Immune infiltration in the tumor microenvironment (TME) is correlated with the clinical prog-

Table 2. Univariate and multivariate analyses of disease-specific survival and overall survival in patients with EOC

Characteristic	DSS					OS				
	Total (N)	HR (95% CI) Univariate analysis	*P* value	HR (95% CI) Multivariate analysis	*P* value	Total (N)	HR (95% CI) Univariate analysis	*P* value	HR (95% CI) Multivariate analysis	*P* value
FIGO stage (Stage III & Stage IV vs. Stage I & Stage II)	347	2.244 (0.922-5.462)	0.075	1.294 (0.311-5.394)	0.723	371	2.085 (0.925-4.699)	0.076	2.546 (0.621-10.443)	0.194
Histologic grade (G3 & G4 vs. G1 & G2)	339	1.313 (0.833-2.070)	0.240			364	1.194 (0.797-1.789)	0.389		
Primary therapy outcome (CR vs. PD & SD & PR)	298	0.227 (0.163-0.317)	< 0.001	0.274 (0.177-0.423)	< 0.001	304	0.234 (0.169-0.324)	< 0.001	0.269 (0.189-0.384)	< 0.001
Anatomic neoplasm subdivision (Bilateral vs. Unilateral)	329	1.034 (0.747-1.431)	0.841			353	1.041 (0.768-1.410)	0.798		
Venous invasion (Yes vs. No)	101	0.846 (0.450-1.591)	0.604			103	0.905 (0.487-1.683)	0.753		
Tumor residual (RD vs. NRD)	310	2.559 (1.572-4.166)	< 0.001	2.203 (1.127-4.307)	0.021	332	2.302 (1.479-3.583)	< 0.001	1.591 (0.949-2.667)	0.078
Age (> 60 vs. ≤ 60)	349	1.282 (0.969-1.695)	0.082	1.580 (1.068-2.338)	0.022	374	1.373 (1.059-1.780)	0.017	1.343 (0.980-1.842)	0.067
Lymphatic invasion (Yes vs. No)	143	1.407 (0.816-2.425)	0.219			147	1.422 (0.839-2.411)	0.191		
TP53 status (Mut vs. WT)	256	0.643 (0.386-1.070)	0.089	0.911 (0.509-1.628)	0.752	273	0.692 (0.423-1.132)	0.143		
PTTG1IP (High vs. Low)	349	1.493 (1.125-1.982)	0.005	1.301 (0.880-1.925)	0.187	374	1.419 (1.091-1.845)	0.009	1.421 (1.029-1.964)	0.033

Abbreviations: FIGO, International Federation of Gynecology and Obstetrics; CR, Complete resolution; PD, Progressive disease; PR, Partial response; SD, Stable disease; NRD, No residual disease; RD, Residual disease; Mut, Mutation; WT, Wild type; PBF, PTTG1-binding factor; EOC, epithelial ovarian cancer; DSS, disease-specific survival.

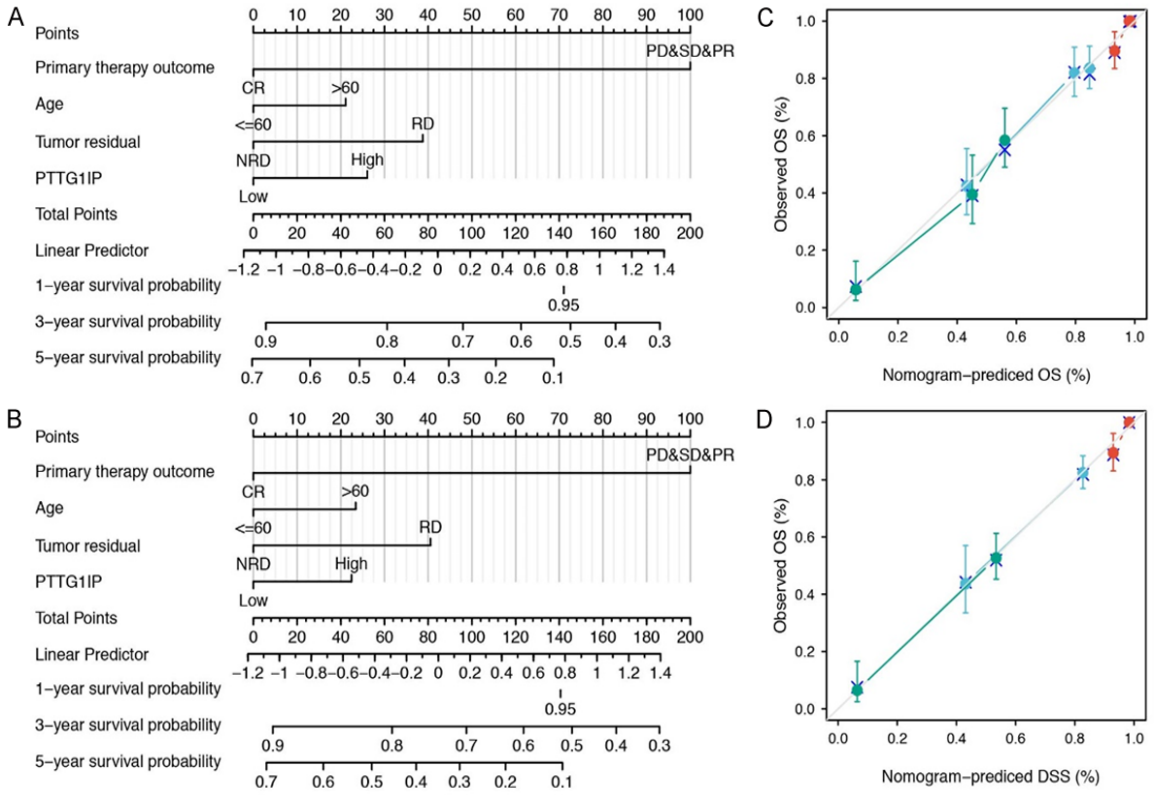

Figure 4. A nomogram combining PBF and other prognostic factors for EOC obtained using TCGA data. The nomograms were constructed as PBF expression-based risk scoring models for (A) 1-, 3-, and 5-year overall survival and (B) disease-specific survival. Calibration plots validating the efficiency of the nomograms for (C) OS and (D) disease-specific survival. PBF, PTTG1-binding factor; EOC, epithelial ovarian cancer; OS, overall survival; OS, overall survival.

nosis of survival in cancers. Therefore, ssGSEA was applied to evaluate the involvement of 24 types of TIICs in the EOC, and Spearman's correlation was used to determine the association between PBF expression and the 24 types of TIICs (**Figure 8A**). The results revealed that PBF expression levels were positively associated with the infiltration levels of the neutrophils (r = 0.298, $P < 0.001$), iDCs (r = 0.303, $P < 0.001$), NK cells (r = 0.305, $P < 0.001$), and Tem (r = 0.410, $P < 0.001$) (**Figure 8B**). In addition, the infiltration levels of the Tgd cells ($P < 0.001$), Th1 cells ($P = 0.012$), NK $CD56^{dim}$ cells ($P = 0.033$), neutrophils ($P < 0.001$), DCs ($P = 0.005$), eosinophils ($P < 0.001$), iDCs ($P < 0.001$), macrophages ($P < 0.001$), mast cells ($P = 0.007$), NK cells ($P < 0.001$), Tcm ($P = 0.019$), and Tem ($P < 0.001$) were considerably enriched in the PBF-high group (**Figure 8C**). Altogether these results suggest that PBF affects immune cell infiltration in EOC.

Prognostic value of PBF expression in EOC based on the TIIC subsets

The role of TIIC for the prognosis of EOC was explored using TIMER, which confirmed that a higher expression of PBF in the DCs cells was associated with the prognosis of EOC (**Figure 9**). However, higher expression of PBF was not associated with any obvious differences in the survival in B cells, $CD8^+$ T cells, $CD4^+$ T cells, macrophages, and neutrophils of patients with EOC ($P > 0.05$), which verified that high PBF expression in EOC affected prognosis partly due to TIIC levels.

PBF expression correlates with immune markers

To confirm a correlation between PBF expression and immune infiltration, we explored the association between PBF and multiple immune marker genes of diversified immune cells, su-

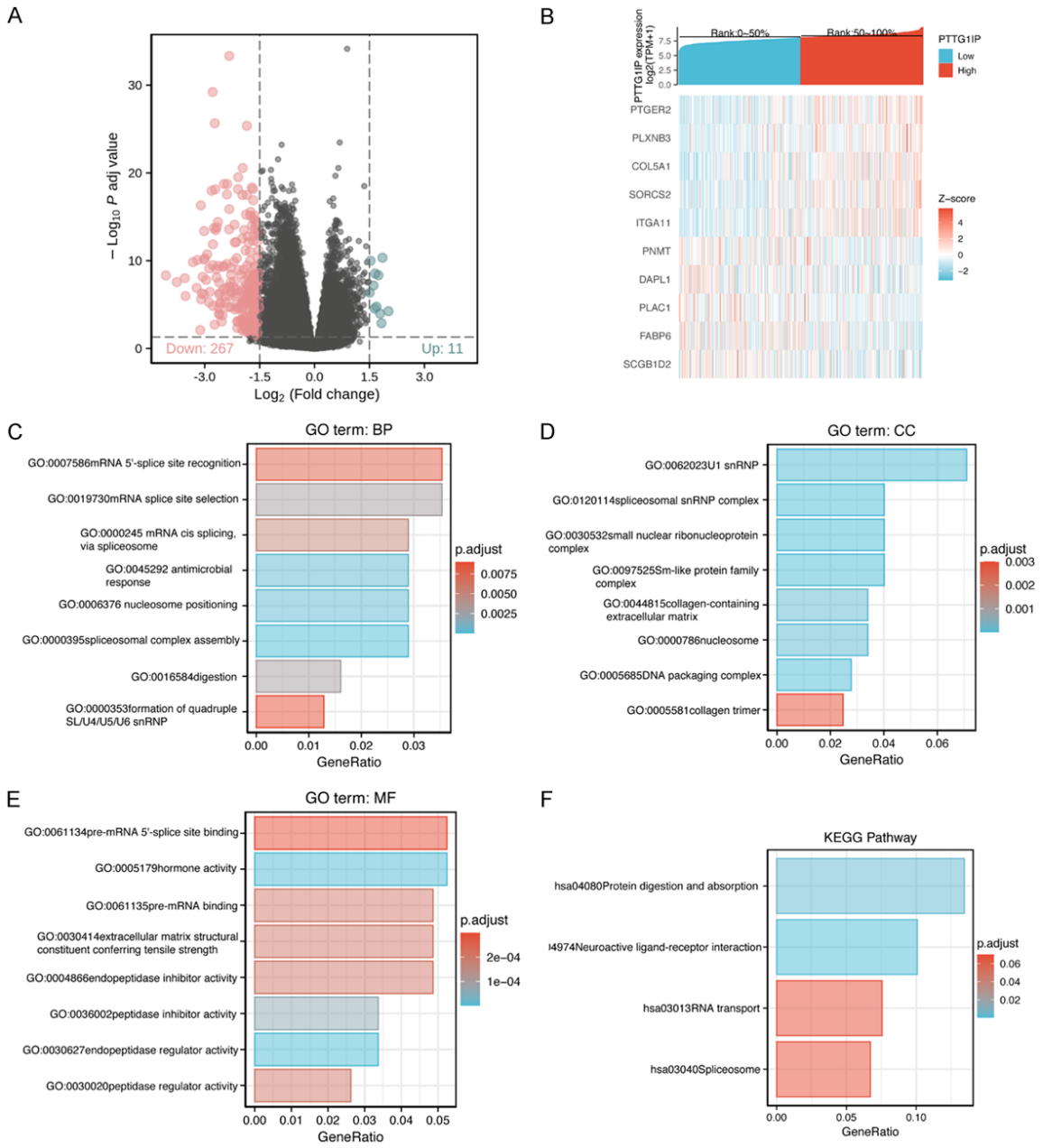

Figure 5. A. Volcano Plots of the DEGs; B. Heatmap of the DEGs. C-E. Gene Ontology (GO) analysis showing the top eight genes each for biological processes (BP), cellular components (CC), and molecular functions (MF). F. KEGG pathway analysis and the top eight pathways mapped based on genes co-expressed with NLRP12.

ch as B cells, neutrophils, $CD8^+$ T cells, T cells (general), TAMs, monocytes, and DCs in EOC, using TIMER. Moreover, multiple functional T cells, including Th1 cells, Th2 cells, Th17 cells, and exhausted T cells were explored. After the correlation adjustment for purity, we noticed that the PBF expression level was significantly linked with most immune marker sets of the diverse immune cells and multiple T cells in EOC (**Table 3**). Overall, the results showed a close relationship between PBF and immune cell infiltration in EOC.

Discussion

As an oncogenic protein, pituitary tumor transforming gene 1 binding factor (PTTG1IP, also called PBF) actively participates in the meta-

A BIOCARTA_P53_PATHWAY

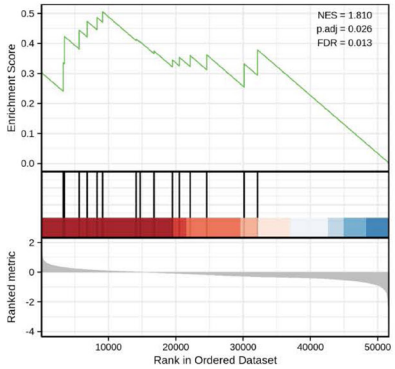

B REACTOME_SUMOYLATION_OF_DNA_DAMAGE_RESPONSE_AND_REPAIR_PROTEINS

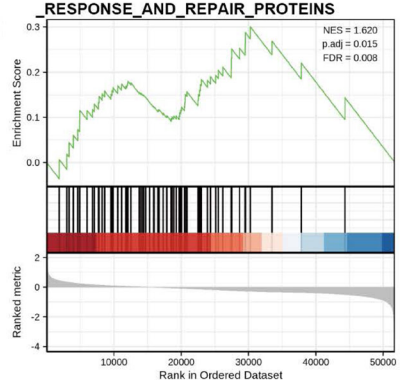

C SA_B_CELL_RECEPTOR_COMPLEXES

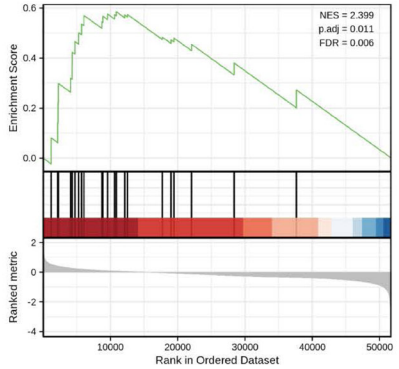

D BIOCARTA_TOLL_PATHWAY

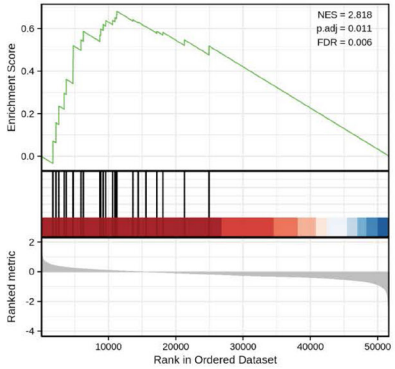

E REACTOME_SIGNALING_BY_WNT_IN_CANCER

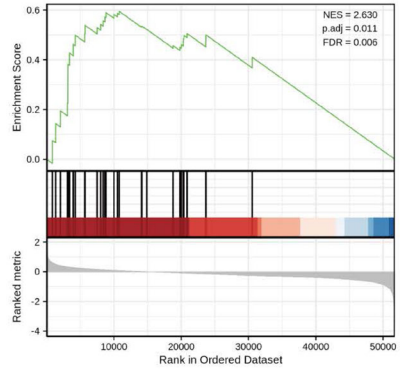

F REACTOME_AKT_PHOSPHORYLATES_TARGETS_IN_THE_NUCLEUS

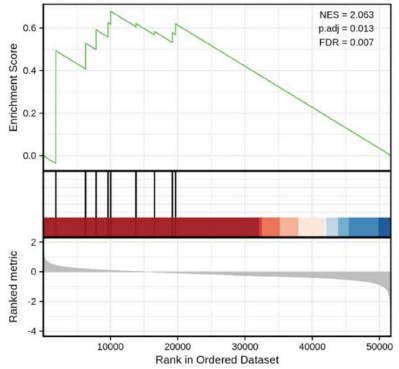

G REACTOME_ESTROGEN_DEPENDENT_NUCLEAR_EVENTS_DOWNSTREAM_OF_ESR_MEMBRANE_SIGNALING

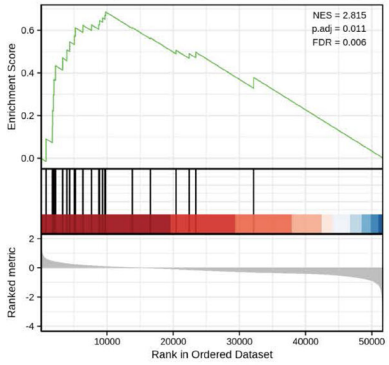

H REACTOME_CELL_EXTRACELLULAR_MATRIX_INTERACTIONS

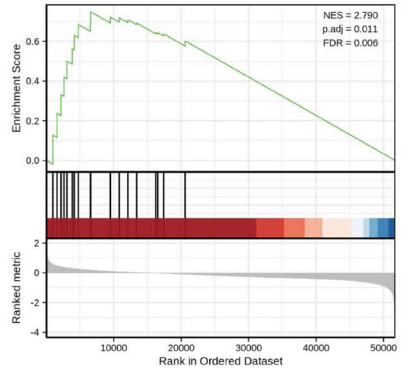

I PID_FGF_PATHWAY

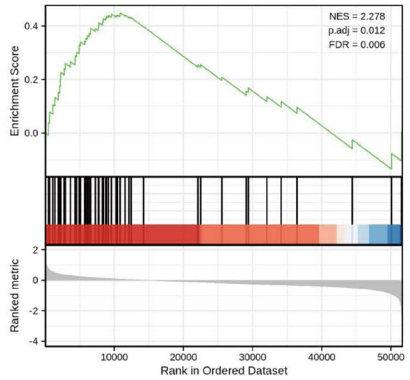

Figure 6. Enrichment plots obtained using GSEA data. PBF was differentially enriched in the (A) P53 pathway, (B) DNA damage replication, (C) B cell receptor complexes, (D) Toll pathway, (E) Wnt signaling pathway, (F) Akt phosphorylation pathway, (G) estrogen dependent nuclear pathway, (H) extracellular matrix interaction, and (I) FGF pathway.

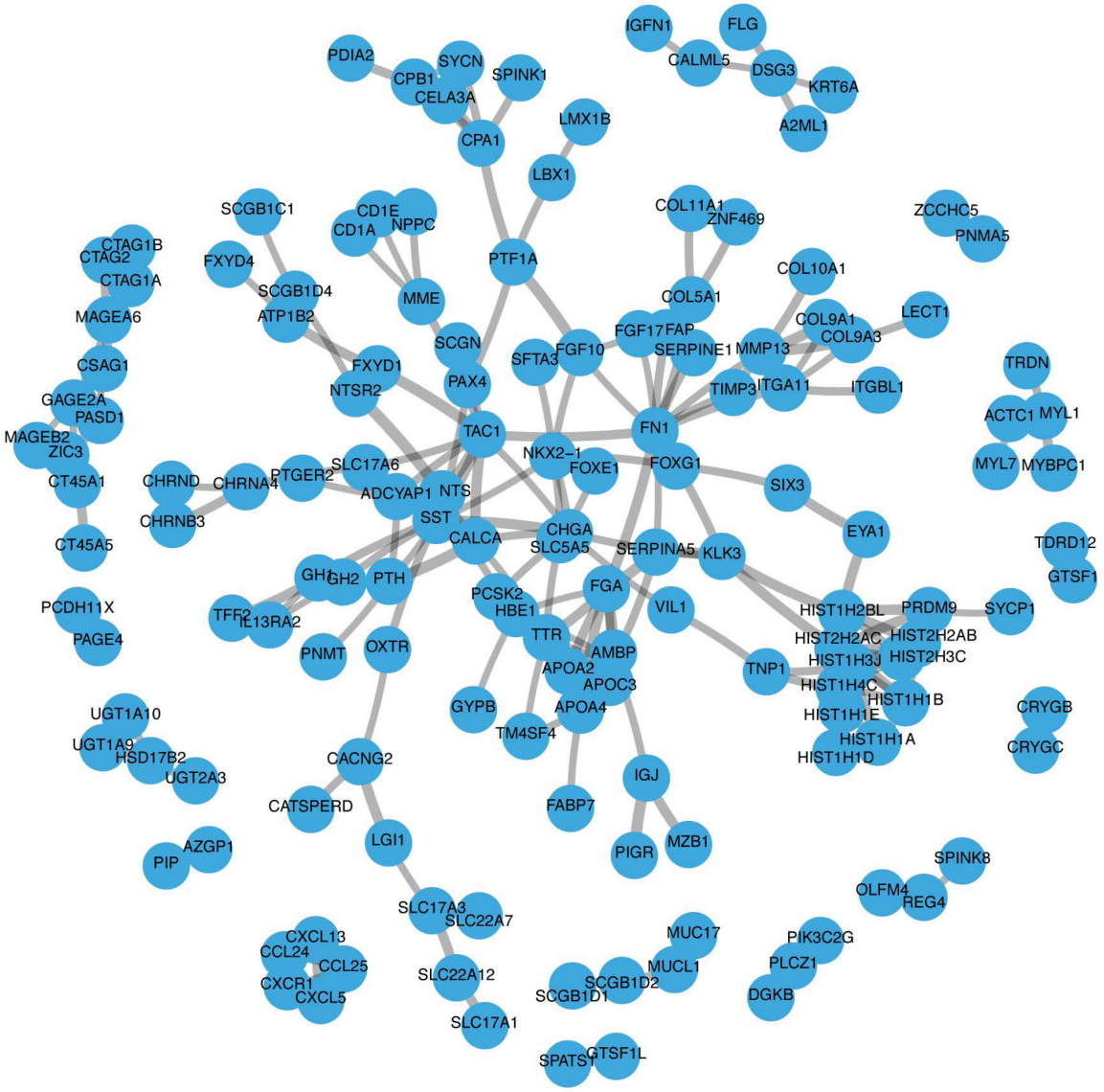

Figure 7. The protein-protein interaction (PPI) network was construction based on PBF co-expression genes. PBF, PTTG1-binding factor.

phase-anaphase transition of the cell cycle through the activation of securin (PTTG1). The expression of PBF has been identified in many tumors including thyroid, pituitary, and breast [8, 12]. Higher PBF expression is associated with early tumor recurrence in thyroid cancer [12]. Functional studies conducted on breast cancer and colorectal carcinoma cells have demonstrated that PBF overexpression promotes cell invasion [11, 14]. Collectively, these observations suggest that PBF may be involved in tumorigenesis, but its precise role in EOC development and progression have not been comprehensively studied.

In our study, clinical information download from the TCGA database was used to evaluated PBF expression in different types of cancers, and

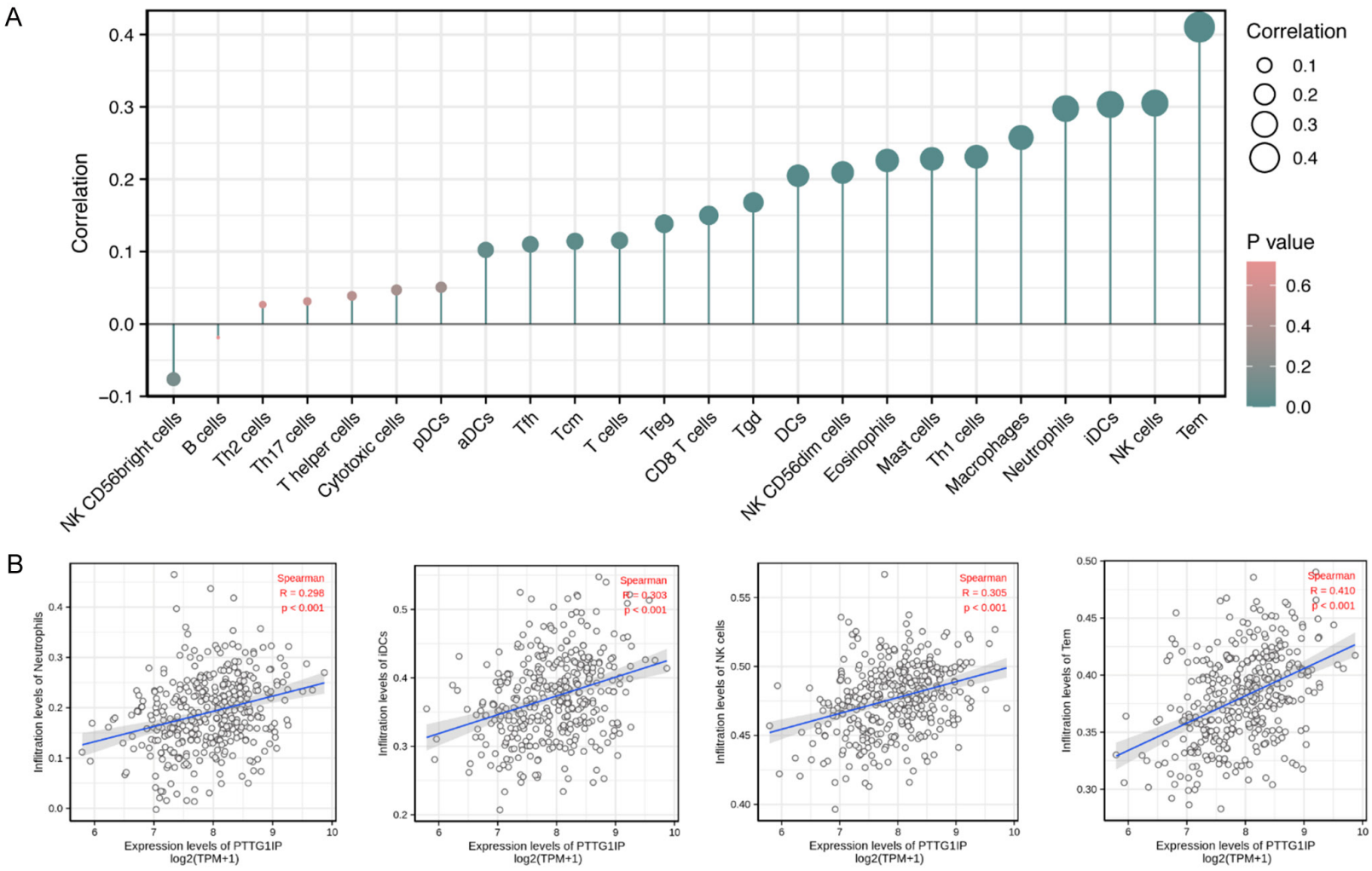
A
Correlation
0.4
0.3
0.2
0.1
0.0
−0.1
NK CD56bright cells
B cells
Th2 cells
Th17 cells
T helper cells
Cytotoxic cells
pDCs
aDCs
Tfh
Tcm
T cells
Treg
CD8 T cells
Tgd
DCs
NK CD56dim cells
Eosinophils
Mast cells
Th1 cells
Macrophages
Neutrophils
iDCs
NK cells
Tem
Correlation
0.1
0.2
0.3
0.4
P value
0.6
0.4
0.2
0.0
B
Infiltration levels of Neutrophils
Spearman
R = 0.298
p < 0.001
Infiltration levels of iDCs
Spearman
R = 0.303
p < 0.001
Infiltration levels of NK cells
Spearman
R = 0.305
p < 0.001
Infiltration levels of Tem
Spearman
R = 0.410
p < 0.001
Expression levels of PTTG1IP
log2(TPM+1)

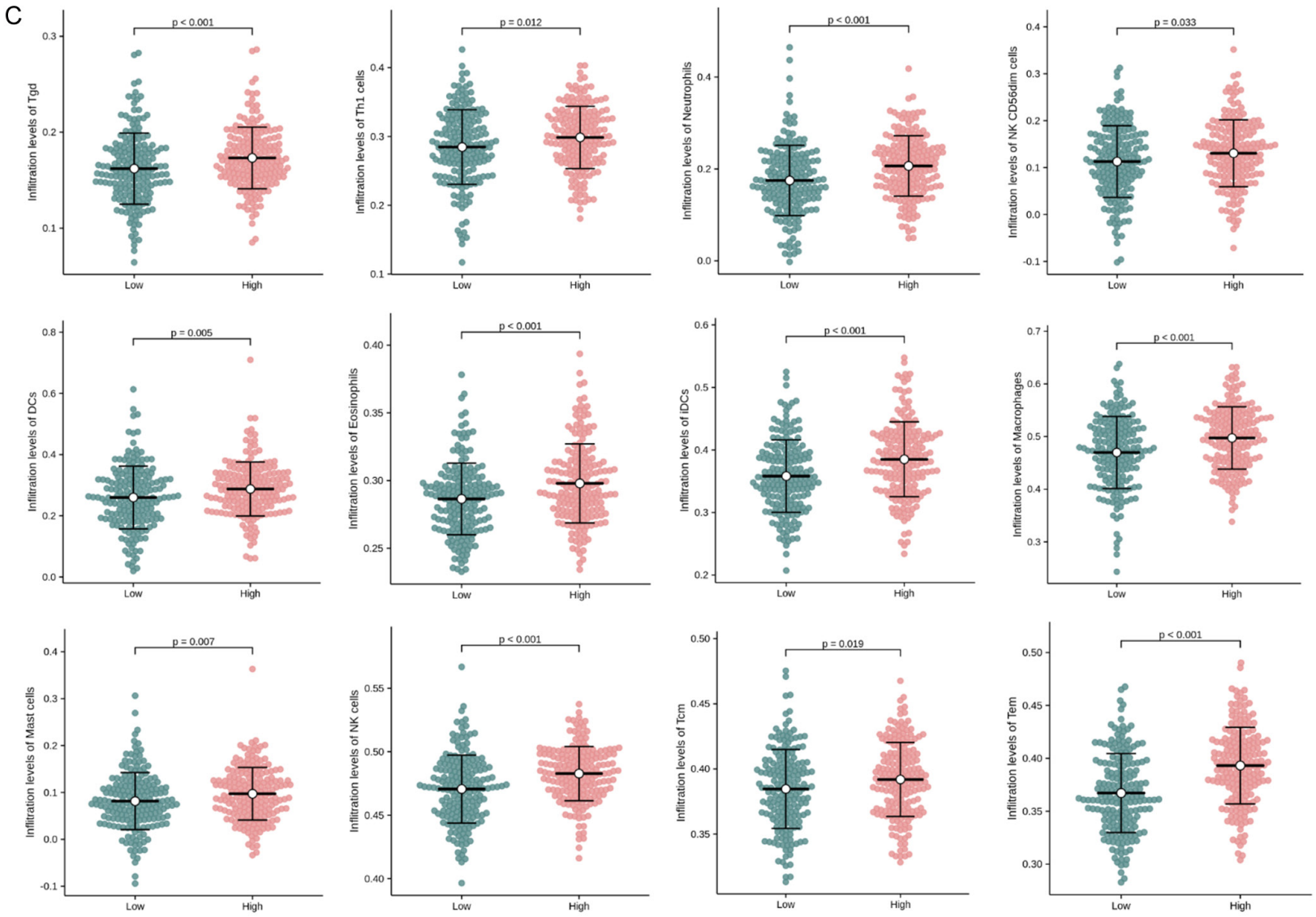

Figure 8. ssGSEA analyses of PBF and the association between PBF expression and immune infiltration level in EOC. A. The correlation between the infiltration of immune cells and the expression of PBF; B. PBF expression was prominently positively associated with the infiltration levels of neutrophils, iDC cells, NK cells, and Tem cells; C. The infiltration levels of Tgd cells, neutrophils cells, NK CD56dim cells, eosinophils, iDCs, DCs, eosinophils, neutrophils, iDCs cells, macrophages cells, mast cells, NK cells, Tcm cells, and Tem cells were significantly higher in the PBF-high expression group. PBF, PTTG1-binding factor; EOC, epithelial ovarian cancer.

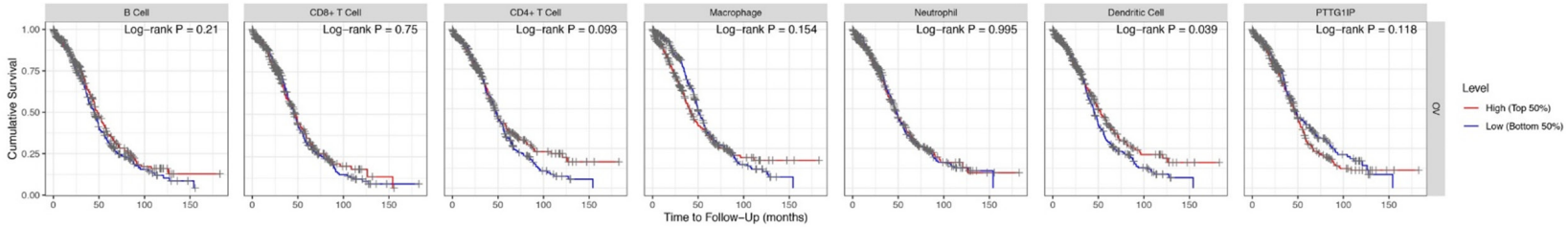

Figure 9. Comparison of the Kaplan-Meier survival curves of the high and low PBF expression groups in EOC based on immune cell subgroups analysis conducted using TIMER. PBF, PTTG1-binding factor; EOC, epithelial ovarian cancer.

Table 3. Correlation analysis between PBF and related gene markers of immune cells in EOC by TIMER

Description	Gene marker	None		Purity	
		Cor	p	Cor	p
B cell	CD19	-0.114	4.76e-02	-0.144	2.34e-02
	CD79A	-0.01	8.68e-01	-0.159	1.21e-02
$CD8^+$ T cell	CD8A	-0.134	1.95e-02	-0.012	8.55e-01
	CD8B	0.1	8.32e-02	-0.002	9.72e-01
Dendritic cell	ITGAX	0.275	1.31e-06	0.123	5.25e-02
	NRP1	0.295	1.62e-07	0.182	4.00e-03
	CD1C	0.185	1.2e-03	0.006	3.03e-04
	HLA-DPA1	0.131	2.23e-02	-0.007	9.07e-01
	HLA-DRA	0.116	4.29e-02	0.008	8.96e-01
	HLA-DQB1	0.057	3.21e-01	-0.082	1.99e-01
	HLA-DPB1	0.171	2.92e-03	0.034	5.89e-01
M1 Macrophage	PTGS2	0.148	9.67e-03	0.037	5.58e-01
	IRF5	0.136	1.76e-02	0.043	5.02e-01
	NOS2	0.095	9.84e-02	0.006	2.99e-01
M2 Macrophage	MS4A4A	0.222	1.04e-04	0.053	4.03e-01
	VSIG4	0.225	8.14e-05	0.054	3.93e-01
	CD163	0.261	4.33e-06	0.1	1.17e-01
Monocyte	CSF1R	0.295	1.67e-07	0.126	4.66e-02
	CD86	0.214	1.83e-04	0.036	5.76e-01
Natural killer cell	KIR2DS4	0.151	8.56e-03	0.074	2.46e-01
	KIR3DL3	0.014	7.95e-01	-0.02	7.59e-01
	KIR3DL2	0.143	1.27e-02	0.069	2.78e-01
	KIR3DL1	0.11	5.55e-02	-0.008	9.04e-01
	KIR2DL4	0.094	1.02e-01	-0.019	7.64e-01
	KIR2DL3	0.195	6.44e-04	0.144	2.29e-02
	KIR2DL1	0.136	1.8e-02	0.088	1.66e-01
Neutrophils	CCR7	0.123	3.29e-02	-0.037	5.64e-01
	ITGAM	0.288	3.66e-07	0.103	1.05e-01
	CEACAM8	0.08	1.64e-01	0.007	2.23e-01
T cell (general)	CD3D	0.098	8.71e-02	-0.086	1.78e-01
	CD3E	0.151	8.37e-03	-0.028	6.65e-01
T cell exhaustion	CTLA4	0.116	4.3e-02	-0.035	5.78e-01
	LAG3	-0.02	7.29e-01	-0.13	4.05e-02
	HAVCR2	0.246	1.64e-05	0.066	2.99e-01
	GZMB	0.057	8.2e-01	-0.092	1.49e-01
	PDCD1	0.141	1.41e-02	0.008	8.97e-01
TAM	CCL2	0.154	7.15e-03	-0.028	6.60e-01
	IL10	0.275	1.28e-06	0.148	1.98e-02
	CD68	0.231	5.3e-05	0.064	3.15e-01
Tfh	BCL6	0.099	8.39e-02	0.117	6.48e-02
	IL21	-0.056	3.34e-01	-0.045	4.82e-01
Th1	TBX21	0.129	2.45e-02	-0.055	3.86e-01
	STAT4	0.184	1.27e-03	0.071	2.65e-01
	STAT1	0.082	1.56e-01	0.084	1.84e-01
	IFNG	0.047	4.11e-01	-0.074	2.44e-01
	IL13	0.08	1.66e-01	0.066	2.98e-01

found that PBF expression was enhanced in a diverse range of cancers compared with corresponding normal tissues, and in particular in EOC, as its high expression was identified in EOC using the GSE40595 dataset and the HPA. Further clinical validation also suggested that PBF was overexpressed in the EOC cell lines and EOC tissues obtained from the PKUPH database, which is in line with previous studies that showed that PBF is highly expressed in various types of cancer, including thyroid cancer, prostate cancer, and head and neck squamous cell carcinoma. PBF and PTTG greatly promote thyroid cancer, which make them candidate biomarkers for prognosis and therapy in EOC patients [12]. Previous immunohistochemical results have demonstrated that PBF expression was higher in prostate cancer than in benign prostatic hyperplasia or adjacent normal prostate specimens [16]. These results are similar to our findings with EOC obtained from TCGA, indicating that PBF may be a diagnostic marker in multiple cancers.

The high expression of PBF in EOC indicates poor prognosis. This study showed that PBF overexpression was associated with clinical values, such as primary therapy outcome, residual tumor, and age. In addition, the Kaplan-Meier survival analysis confirmed that high PBF expression was associated with a worse DSS and OS in EOC based on TCGA data. These studies have highlighted that PBF expression is associated with the clinical features and the survival of EOC patients, and may serve as a prognostic biomarker. Additionally, the univariate Cox analysis conducted on TCGA data showed that PBF expression is a prognostic factor in EOC. Similarly, head and neck squamous cell carcinoma patients with high PBF expression had the

Th2	GATA3	0.219	1.29e-04	0.101	1.12e-01
	STAT6	0.158	5.94e-03	0.161	1.08e-02
	STAT5A	0.084	1.45e-01	0.041	5.21e-01
Th17	STAT3	0.292	2.52e-07	0.238	1.53e-04
	IL17A	0.065	2.57e-01	-0.003	9.58e-01
Treg	FOXP3	0.197	5.63e-04	0.093	1.45e-01
	CCR8	0.178	1.86e-03	0.071	2.67e-01
	STAT5B	0.121	3.6e-02	0.09	1.59e-01
	TGFB1	0.337	2.12e-09	0.217	5.81e-04

Abbreviations: PBF, PTTG1-binding factor; EOC, epithelial ovarian cancer.

poorest OS [17]. The multivariate analysis demonstrated that PBF expression was an independent survival biomarker of DSS and OS in EOC patients. Overall, the results of the analyses confirmed that PBF expression may be a useful prognostic biomarker in EOC. High PBF expression was associated with an unsatisfactory prognosis of stage III-IV and G3 subgroups of EOC patients, with the highest HR associated with the lowest OS and DSS. It was observed that PBF expression was an effective prognostic biomarker in all subsets, indicating that PBF is an independent clinicopathological value.

Given that PBF is a significant prognostic factor, we created a nomogram, in which PBF is a prognostic marker for EOC. The results of the multivariate Cox analysis were used to construct a nomogram with PBF being an independent factor of clinical risk (primary therapy outcome, tumor residual and age). In TCGA cohorts, the C-indexes and calibration plots demonstrated that the nomogram performed well in predicting the 1-, 3-, 5-year OS and DSS in patients with EOC, and provided a personalized score that could be used to identify high-risk EOC patients and provide them with more aggressive therapy regimens.

To verify the molecular mechanism of PBF in EOC, we implemented the GSEA to analyze the pathways that were upregulated under PBF expression. The results showed that PBF may be involved in multiple signaling pathways, including DNA damage replication, P53 pathway, B cell receptor complexes, Wnt signaling pathway, Akt phosphorylates pathway, and estrogen dependent nuclear pathway. Certain studies have revealed that PBF may affect several biologic functions, including cell transformation, migration, and invasion [11, 18, 19]. For instance, head and neck squamous cell carcinoma patients with high PBF suffered a worse outcome partially due to greater aberration of the p53-dependent signaling pathway [17]. Previous research has demonstrated that PBF may be a prognostic indicator in invasive tumors through its regulation of p53 activity in colorectal tumorigenesis [11]. It was also reported that as a proto-oncogene, PBF may serve as a negative regulator of p53 function in thyroid tumorigenesis [20]. Evidence has also indicated that PBF and PTTG play a crucial role in regulating genes associated with DNA damage response, which is related to poor clinical outcome [12]. Functional regulatory variants of PBF have been associated with the risk of developing ER-positive breast cancer, which was then confirmed through its function as a proto-oncogene in breast cancer [10]. PBF over-expression activates PI3K/Akt signaling and may contribute to enhance the vulnerability of females towards thyroid disease [13]. In general, these results verified that PBF is strongly associated with tumorigenesis. Therefore, PBF may affect the carcinogenesis of EOC by regulating these signaling pathways, leading to a more unsatisfactory prognosis in EOC patients.

In recent years, many studies have revealed that TIICs can regulate the development and progression of tumors, and immune cell infiltration exerts an influence on the survival of EOC patients [21]. In our study, the ssGSEA analysis was used to examine the association between PBF expression and immune cell infiltration in EOC. By analyzing an estimated fraction of the 24 TIICs in EOC, we found that PBF expression was positively associated with the infiltration levels of the iDCs, neutrophils, NK cells, and Tem. Infiltrating NK cells exert a strong immunosuppressive effect on the tumor microenvironment, reducing the secretion of IFN-γ and inducing T cell dysfunction [22]. Neutrophils play an essential role in innate immunity, which initiates an adaptive immune system response towards antigen stimuli. Simultaneously, neutrophils are also possible immunotherapy targets [23]. The analysis results proved that PBF

may play a role in the recruitment and activation of CTLs by neutrophils. In addition, PBF is associated with most immune markers in EOC, such as $CD8^+$ T cells and T cells, indicating that PBF may affect the regulation of T cell responses. Furthermore, PBF was highly associated with other T-cell markers, such as the different subtypes of T-helper cells in EOC, which indicated that PBF may regulate T lymphocyte immunity in EOC. PBF was also negatively associated with B cell markers (CD19 and CD79a) and TAM markers (CCL2), which suggests that it may affect immunosuppression and the regulation of macrophage polarization in EOC. The weak relationship between PBF and M1/M2 macrophage markers, such as PTGS2, IRF5, CD163, VSIG4, CD163, and MS4A4A, suggests that PBF affects the regulation of TAM polarization. Furthermore, PBF was associated with T cell exhaustion markers (PDCD1, CTLA4, LAG3, HAVCR2 and GZMB) and Treg markers (FOXP3, CCR8, STAT5B and TGFB1), which verified that PBF may influence immune escape in EOC. Together, these analysis results prove that PBF is associated with immune cell infiltration, which may serve as a novel immunotherapy target during EOC development, that affects the prognosis of EOC patients. Further studies are required to expound the relevant mechanisms between immune cell infiltration and PBF.

Our study, which was based on preliminary data obtained from TCGA has certain limitations. First, the sample size in the cohort study of EOC was relatively small, and more precise data can be obtained using a larger sample size and sufficient clinical information. Second, the possible regulatory mechanisms of PBF in EOC need to be further validated. Furthermore, more efforts are required to further illustrate the mechanisms involved in PBF-related immune infiltration for the development of immunotherapies for EOC.

In brief, this study verified that PBF may act as a promising biomarker and a marker of poor prognosis in EOC. Additionally, a strong correlation between PBF and pathways in EOC, such as the P53 pathway, B cell receptor pathway, toll pathway, Wnt pathway, FGF pathway, and Akt phosphorylation, was observed. Furthermore, PBF may also affect the microenvironment of EOC by regulating the tumor-infiltration of immune cells, indicating that PBF is a therapeutic target that regulates anti-tumor immune response. High PBF expression may be an independent prognostic factor for EOC patients and might be developed as a novel therapeutic target for EOC patients.

Disclosure of conflict of interest

None.

Address correspondence to: Jianliu Wang, Department of Obstetrics and Gynecology, Peking University People's Hospital, Xizhimen South Street, Beijing 100044, China. E-mail: wangjianliu@pkuph.edu.cn

References

[1] Siegel RL, Miller KD and Jemal A. Cancer statistics, 2020. CA Cancer J Clin 2020; 70: 7-30.

[2] Ghoneum A, Afify H, Salih Z, Kelly M and Said N. Role of tumor microenvironment in the pathobiology of ovarian cancer: insights and therapeutic opportunities. Cancer Med 2018; 7: 5047-5056.

[3] Corvigno S, Mezheyeuski A, De La Fuente LM, Westbom-Fremer S, Carlson JW, Fernebro J, Avall-Lundqvist E, Kannisto P, Hedenfalk I, Malander S, Rolny C, Dahlstrand H and Ostman A. High density of stroma-localized CD11c-positive macrophages is associated with longer overall survival in high-grade serous ovarian cancer. Gynecol Oncol 2020; 159: 860-868.

[4] Gonzalez-Pastor R, Goedegebuure PS and Curiel DT. Understanding and addressing barriers to successful adenovirus-based virotherapy for ovarian cancer. Cancer Gene Ther 2021; 28: 375-389.

[5] Mirza MR, Benigno B, Dorum A, Mahner S, Bessette P, Barcelo IB, Berton-Rigaud D, Ledermann JA, Rimel BJ, Herrstedt J, Lau S, du Bois A, Herraez AC, Kalbacher E, Buscema J, Lorusso D, Vergote I, Levy T, Wang P, de Jong FA, Gupta D and Matulonis UA. Long-term safety in patients with recurrent ovarian cancer treated with niraparib versus placebo: results from the phase III ENGOT-OV16/NOVA trial. Gynecol Oncol 2020; 159: 442-448.

[6] Bantie L, Tadesse S, Likisa J, Yu M, Noll B, Heinemann G, Lokman NA, Ricciardelli C, Oehler MK, Beck A, Pradhan R, Milne R, Albrecht H and Wang S. A first-in-class CDK4 inhibitor demonstrates in vitro, ex-vivo and in vivo efficacy against ovarian cancer. Gynecol Oncol 2020; 159: 827-838.

[7] Liu L, Cai S, Han C, Banerjee A, Wu D, Cui T, Xie G, Zhang J, Zhang X, McLaughlin E, Yin M, Backes FJ, Chakravarti A, Zheng Y and Wang QE. ALDH1A1 contributes to PARP inhibitor re-

sistance via enhancing DNA repair in BRCA2(-/-) ovarian cancer cells. Mol Cancer Ther 2020; 19: 199-210.

[8] Repo H, Gurvits N, Loyttyniemi E, Nykanen M, Lintunen M, Karra H, Kurki S, Kuopio T, Talvinen K, Soderstrom M and Kronqvist P. PTTG1-interacting protein (PTTG1IP/PBF) predicts breast cancer survival. BMC Cancer 2017; 17: 705.

[9] Chien W and Pei L. A novel binding factor facilitates nuclear translocation and transcriptional activation function of the pituitary tumor-transforming gene product. J Biol Chem 2000; 275: 19422-19427.

[10] Xiang C, Gao H, Meng L, Qin Z, Ma R, Liu Y, Jiang Y, Dang C, Jin L, He F and Wang H. Functional variable number of tandem repeats variation in the promoter of proto-oncogene PTTG1IP is associated with risk of estrogen receptor-positive breast cancer. Cancer Sci 2012; 103: 1121-1128.

[11] Read ML, Seed RI, Modasia B, Kwan PP, Sharma N, Smith VE, Watkins RJ, Bansal S, Gagliano T, Stratford AL, Ismail T, Wakelam MJ, Kim DS, Ward ST, Boelaert K, Franklyn JA, Turnell AS and McCabe CJ. The proto-oncogene PBF binds p53 and is associated with prognostic features in colorectal cancer. Mol Carcinog 2016; 55: 15-26.

[12] Read ML, Fong JC, Modasia B, Fletcher A, Imruetaicharoenchoke W, Thompson RJ, Nieto H, Reynolds JJ, Bacon A, Mallick U, Hackshaw A, Watkinson JC, Boelaert K, Turnell AS, Smith VE and McCabe CJ. Elevated PTTG and PBF predicts poor patient outcome and modulates DNA damage response genes in thyroid cancer. Oncogene 2017; 36: 5296-5308.

[13] Read ML, Lewy GD, Fong JC, Sharma N, Seed RI, Smith VE, Gentilin E, Warfield A, Eggo MC, Knauf JA, Leadbeater WE, Watkinson JC, Franklyn JA, Boelaert K and McCabe CJ. Proto-oncogene PBF/PTTG1IP regulates thyroid cell growth and represses radioiodide treatment. Cancer Res 2011; 71: 6153-6164.

[14] Watkins RJ, Read ML, Smith VE, Sharma N, Reynolds GM, Buckley L, Doig C, Campbell MJ, Lewy G, Eggo MC, Loubiere LS, Franklyn JA, Boelaert K and McCabe CJ. Pituitary tumor transforming gene binding factor: a new gene in breast cancer. Cancer Res 2010; 70: 3739-3749.

[15] Tan X, Zhang S, Gao H, He W, Xu M, Wu Q, Ni X and Jiang H. Hypermethylation of the PTTG1IP promoter leads to low expression in early-stage non-small cell lung cancer. Oncol Lett 2019; 18: 1278-1286.

[16] Huang SQ, Wang B, Liao QJ, Shen CX and Li WB. Pituitary tumor transforming gene binding factor (PBF) is required for androgen-induced prostate cancer proliferation and invasion. Neoplasma 2019; 66: 327-335.

[17] Read ML, Modasia B, Fletcher A, Thompson RJ, Brookes K, Rae PC, Nieto HR, Poole VL, Roberts S, Campbell MJ, Boelaert K, Turnell AS, Smith VE, Mehanna H and McCabe CJ. PTTG and PBF functionally interact with p53 and predict overall survival in head and neck cancer. Cancer Res 2018; 78: 5863-5876.

[18] Stratford AL, Boelaert K, Tannahill LA, Kim DS, Warfield A, Eggo MC, Gittoes NJ, Young LS, Franklyn JA and McCabe CJ. Pituitary tumor transforming gene binding factor: a novel transforming gene in thyroid tumorigenesis. J Clin Endocrinol Metab 2005; 90: 4341-4349.

[19] Watkins RJ, Imruetaicharoenchoke W, Read ML, Sharma N, Poole VL, Gentilin E, Bansal S, Bosseboeuf E, Fletcher R, Nieto HR, Mallick U, Hackshaw A, Mehanna H, Boelaert K, Smith VE and McCabe CJ. Pro-invasive effect of proto-oncogene PBF is modulated by an interaction with cortactin. J Clin Endocrinol Metab 2016; 101: 4551-4563.

[20] Read ML, Seed RI, Fong JC, Modasia B, Ryan GA, Watkins RJ, Gagliano T, Smith VE, Stratford AL, Kwan PK, Sharma N, Dixon OM, Watkinson JC, Boelaert K, Franklyn JA, Turnell AS and McCabe CJ. The PTTG1-binding factor (PBF/PTTG1IP) regulates p53 activity in thyroid cells. Endocrinology 2014; 155: 1222-1234.

[21] Yan S, Fang J, Chen Y, Xie Y, Zhang S, Zhu X and Fang F. Comprehensive analysis of prognostic gene signatures based on immune infiltration of ovarian cancer. BMC Cancer 2020; 20: 1205.

[22] Platonova S, Cherfils-Vicini J, Damotte D, Crozet L, Vieillard V, Validire P, Andre P, Dieu-Nosjean MC, Alifano M, Regnard JF, Fridman WH, Sautes-Fridman C and Cremer I. Profound coordinated alterations of intratumoral NK cell phenotype and function in lung carcinoma. Cancer Res 2011; 71: 5412-5422.

[23] Kargl J, Busch SE, Yang GH, Kim KH, Hanke ML, Metz HE, Hubbard JJ, Lee SM, Madtes DK, McIntosh MW and Houghton AM. Neutrophils dominate the immune cell composition in non-small cell lung cancer. Nat Commun 2017; 8: 14381.

Supplementary Table 1. Clinical characteristics of ovarian cancer patients based on TCGA

Characters	level	Overall
n		376
FIGO stage (%)	Stage I	1 (0.3%)
	Stage II	22 (5.9%)
	Stage III	293 (78.6%)
	Stage IV	57 (15.3%)
Histologic grade (%)	G1	1 (0.3%)
	G2	42 (11.5%)
	G3	322 (88%)
	G4	1 (0.3%)
Primary therapy outcome (%)	CR	213 (69.8%)
	PD	27 (8.9%)
	PR	43 (14.1%)
	SD	22 (7.2%)
Anatomic neoplasm subdivision (%)	Bilateral	253 (71.5%)
	Unilateral	101 (28.5%)
Venous invasion (%)	No	40 (38.8%)
	Yes	63 (61.2%)
Tumor residual (%)	NRD	66 (19.8%)
	RD	267 (80.2%)
Lymphatic invasion (%)	No	48 (32.4%)
	Yes	100 (67.6%)
TP53 status (%)	Mut	248 (90.5%)
	WT	26 (9.5%)
Age (%)	≤ 60	207 (55.1%)
	> 60	169 (44.9%)
Age (median [IQR])		60.00 [52.00, 70.00]

Supplementary Table 2. Relationship between PBF expression and clinical pathological characteristics based on the logistics regression analysis

Characteristics	Odds Ratio in PTTG1IP expression	Odds Ratio (OR)	*P* value
FIGO stage (Stage III & Stage IV vs. Stage I & Stage II)	373	1.59 (0.68-3.91)	0.291
Histologic grade (G3 & G4 vs. G1 & G2)	366	0.62 (0.32-1.17)	0.147
Primary therapy outcome (CR vs. PD & SD & PR)	305	0.60 (0.36-0.98)	0.043
Anatomic neoplasm subdivision (Bilateral vs. Unilateral)	354	1.46 (0.92-2.33)	0.111
Venous invasion (Yes vs. No)	103	1.22 (0.55-2.70)	0.629
Tumor residual (RD vs. NRD)	333	1.99 (1.15-3.51)	0.015
Lymphatic invasion (Yes vs. No)	148	0.96 (0.48-1.92)	0.909
TP53 status (Mut vs. WT)	274	0.94 (0.41-2.12)	0.876

PBF, PTTG1-binding factor; FIGO, International Federation of Gynecology and Obstetrics.

Supplementary Table 3. The prognostic value of PBF (Disease Specific Survival) in each of the ovarian cancer subgroups

Characteristics	N (%)	HR (95% CI)	*P* value
FIGO stage			
Stage I & Stage II	23 (6)	0.282 (0.033-2.429)	0.249
Stage III & Stage IV	348 (94)	1.464 (1.120-1.913)	0.005
Histologic grade			
G1 & G2	43 (12)	1.650 (0.747-3.641)	0.215
G3 & G4	321 (88)	1.420 (1.069-1.885)	0.015

PBF, PTTG1-binding factor.

Supplementary Table 4. The prognostic value of PBF (Overall Survival) in ovarian cancer subgroups

Characteristics	N (%)	HR (95% CI)	*P* value
FIGO stage			
Stage I & Stage II	23 (6)	0.282 (0.033-2.429)	0.249
Stage III & Stage IV	348 (94)	1.464 (1.120-1.913)	0.005
Histologic grade			
G1 & G2	43 (12)	1.650 (0.747-3.641)	0.215
G3 & G4	321 (88)	1.420 (1.069-1.885)	0.015

PBF, PTTG1-binding factor.

Supplementary Table 5. Identification of DEGs between PBF-high and -low groups

gene_id	baseMean	log_2FoldChange	lfcSE	stat	*p* value	padj	gene_name	gene_biotype	cor_*p* value	correlation
ENSG00000198804	920943.0	-0.32070685	0.06382483	-5.0247975	5.039640e-07	7.907464e-06	MT-CO1	protein_coding	3.208138e-01	-0.051319826
ENSG00000210082	847958.6	-0.60857716	0.07514676	-8.0985151	5.563405e-16	1.237003e-13	MT-RNR2	Mt_rRNA	2.334024e-06	-0.241456516
ENSG00000198886	720935.5	-0.41629368	0.06670679	-6.2406493	4.357581e-10	1.834007e-08	MT-ND4	protein_coding	1.860093e-02	-0.121374118
ENSG00000198938	438060.2	-0.50303707	0.07048229	-7.1370703	9.534110e-13	8.168689e-11	MT-CO3	protein_coding	2.049510e-05	-0.218262882
ENSG00000198712	407252.2	-0.54758866	0.07402013	-7.3978340	1.384237e-13	1.550243e-11	MT-CO2	protein_coding	1.688228e-06	-0.244724420
ENSG00000198888	376528.6	-0.45099930	0.07833966	-5.7569727	8.563575e-09	2.384461e-07	MT-ND1	protein_coding	2.830605e-02	-0.113142954
ENSG00000156508	372805.8	-0.17281116	0.07194698	-2.4019239	1.630910e-02	5.069346e-02	EEF1A1	protein_coding	5.125543e-02	0.100622383
ENSG00000198727	345410.6	-0.45623692	0.07556260	-6.0378672	1.561645e-09	5.631435e-08	MT-CYB	protein_coding	3.179599e-02	-0.110778261
ENSG00000198763	339516.3	-0.35279439	0.07401540	-4.7665000	1.874537e-06	2.430127e-05	MT-ND2	protein_coding	2.563859e-01	-0.058660873
ENSG00000075624	330155.2	-0.04273980	0.05146023	-0.8305403	4.062334e-01	5.623849e-01	ACTB	protein_coding	9.037500e-11	0.328036571
ENSG00000111640	304029.2	-0.23810074	0.07209089	-3.3027857	9.572953e-04	4.985658e-03	GAPDH	protein_coding	7.510130e-01	0.016409730
ENSG00000108821	297475.0	0.71359050	0.15459202	4.6159595	3.912832e-06	4.532422e-05	COL1A1	protein_coding	1.408982e-15	0.393338902
ENSG00000198899	236119.5	-0.47002887	0.07206409	-6.5223731	6.920360e-11	3.685011e-09	MT-ATP6	protein_coding	2.698585e-03	-0.154454089
ENSG00000184009	220465.0	0.05847884	0.05610326	1.0423429	2.972527e-01	4.536891e-01	ACTG1	protein_coding	3.941444e-09	0.299082792
ENSG00000019582	215241.3	-0.18699968	0.12412312	-1.5065660	1.319219e-01	2.542341e-01	CD74	protein_coding	4.199569e-04	0.181270726
ENSG00000211459	178026.8	-0.85672836	0.09591804	-8.9318797	4.188306e-19	2.479314e-16	MT-RNR1	Mt_rRNA	2.540869e-08	-0.283553699
ENSG00000120885	174097.6	-0.15339970	0.15092672	-1.0163853	3.094460e-01	4.661684e-01	CLU	protein_coding	8.085836e-02	0.090146848
ENSG00000167244	170040.3	-0.39193194	0.26935335	-1.4550847	1.456458e-01	2.730058e-01	IGF2	protein_coding	2.169393e-01	0.063807890
ENSG00000198786	166149.9	-0.27334687	0.07548629	-3.6211457	2.933013e-04	1.846078e-03	MT-ND5	protein_coding	8.597535e-01	0.009137987
ENSG00000133112	165208.2	-0.47312356	0.08799785	-5.3765353	7.593284e-08	1.557648e-06	TPT1	protein_coding	3.367713e-02	-0.109594447
ENSG00000108107	162878.9	-0.74465080	0.08648893	-8.6097814	7.320003e-18	2.952682e-15	RPL28	protein_coding	2.008589e-07	-0.265171398
ENSG00000161016	160049.2	-0.27710168	0.09018608	-3.0725550	2.122347e-03	9.683678e-03	RPL8	protein_coding	2.257662e-01	-0.062601953
ENSG00000089157	158687.5	-0.35745724	0.07812918	-4.5752077	4.757478e-06	5.371578e-05	RPLP0	protein_coding	1.657116e-02	-0.123561149
ENSG00000149273	157349.1	-0.51247159	0.09086751	-5.6397668	1.702806e-08	4.292898e-07	RPS3	protein_coding	2.070876e-03	-0.158520007
ENSG00000087086	156205.9	-0.25065670	0.07213196	-3.4749741	5.109026e-04	2.942936e-03	FTL	protein_coding	2.654949e-01	0.057552232
ENSG00000105640	153161.8	-0.70170058	0.09358943	-7.4976476	6.497332e-14	7.961153e-12	RPL18A	protein_coding	4.680571e-06	-0.234279587
ENSG00000142541	152479.2	-0.41246740	0.08168527	-5.0494711	4.430350e-07	7.060831e-06	RPL13A	protein_coding	1.302721e-02	-0.128016705
ENSG00000147403	151951.2	-0.32051059	0.08494817	-3.7730135	1.612876e-04	1.107510e-03	RPL10	protein_coding	3.751350e-01	-0.045850669
ENSG00000187244	149810.3	0.05922385	0.10426177	0.5680304	5.700143e-01	7.038284e-01	BCAM	protein_coding	1.098250e-03	0.167900220
ENSG00000140988	146809.2	-0.58136678	0.07804597	-7.4490304	9.402872e-14	1.104619e-11	RPS2	protein_coding	3.226393e-06	-0.238144365
ENSG00000198034	146454.7	-0.40070420	0.08217562	-4.8761935	1.081525e-06	1.530488e-05	RPS4X	protein_coding	4.164723e-02	-0.105130312
ENSG00000231500	140641.5	-0.69521633	0.09889458	-7.0298726	2.067221e-12	1.633033e-10	RPS18	protein_coding	2.578614e-07	-0.262857723
ENSG00000137154	135892.8	-0.55124900	0.08115161	-6.7928288	1.099558e-11	7.099003e-10	RPS6	protein_coding	2.448448e-05	-0.216254416
ENSG00000137818	135613.1	-0.71535345	0.09500061	-7.5299878	5.074507e-14	6.515524e-12	RPLP1	protein_coding	3.754395e-07	-0.259337660
ENSG00000167996	135600.5	0.19647005	0.09340486	2.1034243	3.542869e-02	9.311932e-02	FTH1	protein_coding	6.389048e-09	0.295143744
ENSG00000070756	134209.7	0.03278926	0.07661097	0.4279970	6.686533e-01	7.821279e-01	PABPC1	protein_coding	5.709427e-06	0.232188950

ENSG00000142937	127627.0	-0.50229937	0.08404128	-5.9768172	2.275393e-09	7.715715e-08	RPS8	protein_coding	4.063755e-05	-0.210429708
ENSG00000164692	124614.0	0.66711578	0.13766669	4.8458766	1.260539e-06	1.745871e-05	COL1A2	protein_coding	6.689821e-14	0.375121847
ENSG00000125730	123969.8	0.03104361	0.15115302	0.2053787	8.372763e-01	9.000617e-01	C3	protein_coding	5.392311e-06	0.232792144
ENSG00000167658	122620.8	-0.06458159	0.06925542	-0.9325132	3.510714e-01	5.089106e-01	EEF2	protein_coding	9.252810e-04	0.170354309
ENSG00000167526	122026.1	-0.52346693	0.09656775	-5.4207219	5.935883e-08	1.251487e-06	RPL13	protein_coding	4.013896e-05	-0.210573509
ENSG00000204628	116806.5	-0.32801747	0.07989535	-4.1055890	4.032860e-05	3.387796e-04	GNB2L1	protein_coding	5.971855e-02	-0.097203905
ENSG00000174444	116522.5	-0.28543227	0.07193116	-3.9681311	7.243848e-05	5.614133e-04	RPL4	protein_coding	4.777087e-01	-0.036710424
ENSG00000067225	114185.1	-0.07668766	0.06830061	-1.1227962	2.615241e-01	4.148724e-01	PKM	protein_coding	1.134745e-04	0.198114566
ENSG00000166710	114114.7	-0.11682035	0.09951771	-1.1738650	2.404491e-01	3.911879e-01	B2M	protein_coding	1.276488e-04	0.196655567
ENSG00000197756	113766.1	-0.81744246	0.09169342	-8.9149519	4.880282e-19	2.780602e-16	RPL37A	protein_coding	3.313582e-11	-0.335232914
ENSG00000100316	111821.5	-0.36884589	0.07017551	-5.2560483	1.471837e-07	2.759678e-06	RPL3	protein_coding	1.985311e-01	-0.066441221
ENSG00000008988	111130.5	-0.99739235	0.09492253	-10.5074358	7.983468e-26	2.799188e-22	RPS20	protein_coding	2.454127e-16	-0.397706643
ENSG00000174748	110276.1	-0.42006626	0.07456495	-5.6335620	1.765250e-08	4.430719e-07	RPL15	protein_coding	6.728732e-02	-0.094471246
ENSG00000087460	108476.9	-0.19415220	0.06087338	-3.1894435	1.425470e-03	6.950698e-03	GNAS	protein_coding	1.711086e-01	0.070717309

PBF, PTTG1-binding factor.

Supplementary Table 6. 50 proteins to protein interactions of PBF

node1	node2	node1_external_id	node2_external_id	neighborhood_ on_chromosome	gene_ fusion	phylogenetic_ cooccurrence	coexpression	experimentally_ determined_in- teraction	database_ annotated	automated_ textmining	combined_ score
NTS	NTSR2	9606.ENSP00000256010	9606.ENSP00000303686	0	0.000	0.000	0.063	0.846	0.9	0.896	0.998
NTS	NTSR2	9606.ENSP00000256010	9606.ENSP00000303686	0	0.000	0.000	0.063	0.846	0.9	0.896	0.998
HIST2H2AC	HIST2H2AB	9606.ENSP00000332194	9606.ENSP00000332790	0	0.000	0.000	0.407	0.960	0.9	0.485	0.997
HIST2H2AC	HIST2H2AB	9606.ENSP00000332194	9606.ENSP00000332790	0	0.000	0.000	0.407	0.960	0.9	0.485	0.997
APOC3	APOA2	9606.ENSP00000227667	9606.ENSP00000356969	0	0.000	0.000	0.796	0.000	0.9	0.860	0.996
APOC3	APOA2	9606.ENSP00000227667	9606.ENSP00000356969	0	0.000	0.000	0.796	0.000	0.9	0.860	0.996
COL9A3	COL9A1	9606.ENSP00000341640	9606.ENSP00000349790	0	0.000	0.434	0.641	0.868	0.9	0.846	0.995
COL9A3	COL9A1	9606.ENSP00000341640	9606.ENSP00000349790	0	0.000	0.434	0.641	0.868	0.9	0.846	0.995
HIST1H3J	HIST1H4C	9606.ENSP00000352252	9606.ENSP00000367034	0	0.008	0.000	0.220	0.852	0.9	0.586	0.994
HIST1H3J	HIST1H4C	9606.ENSP00000352252	9606.ENSP00000367034	0	0.008	0.000	0.220	0.852	0.9	0.586	0.994
UGT1A10	UGT1A9	9606.ENSP00000343838	9606.ENSP00000346768	0	0.000	0.000	0.077	0.993	0.0	0.837	0.993
UGT1A10	UGT1A9	9606.ENSP00000343838	9606.ENSP00000346768	0	0.000	0.000	0.077	0.993	0.0	0.837	0.993
PTH	CALCA	9606.ENSP00000282091	9606.ENSP00000331746	0	0.000	0.000	0.000	0.000	0.9	0.927	0.992
PTH	CALCA	9606.ENSP00000282091	9606.ENSP00000331746	0	0.000	0.000	0.000	0.000	0.9	0.927	0.992
PIP	AZGP1	9606.ENSP00000291009	9606.ENSP00000292401	0	0.000	0.000	0.104	0.800	0.9	0.587	0.991
PIP	AZGP1	9606.ENSP00000291009	9606.ENSP00000292401	0	0.000	0.000	0.104	0.800	0.9	0.587	0.991
APOC3	APOA4	9606.ENSP00000227667	9606.ENSP00000350425	0	0.000	0.000	0.565	0.000	0.9	0.789	0.990
APOC3	APOA4	9606.ENSP00000227667	9606.ENSP00000350425	0	0.000	0.000	0.565	0.000	0.9	0.789	0.990

NTS	TAC1	9606.ENSP00000256010	9606.ENSP00000321106	0	0.000	0.000	0.063	0.000	0.9	0.890	0.988
NTS	TAC1	9606.ENSP00000256010	9606.ENSP00000321106	0	0.000	0.000	0.063	0.000	0.9	0.890	0.988
CXCR1	CXCL5	9606.ENSP00000295683	9606.ENSP00000296027	0	0.000	0.000	0.085	0.313	0.9	0.776	0.984
CXCR1	CXCL5	9606.ENSP00000295683	9606.ENSP00000296027	0	0.000	0.000	0.085	0.313	0.9	0.776	0.984
SERPINE1	FN1	9606.ENSP00000223095	9606.ENSP00000346839	0	0.000	0.000	0.295	0.000	0.9	0.735	0.979
SERPINE1	FN1	9606.ENSP00000223095	9606.ENSP00000346839	0	0.000	0.000	0.295	0.000	0.9	0.735	0.979
HIST2H2AC	HIST1H2BL	9606.ENSP00000332194	9606.ENSP00000366618	0	0.000	0.000	0.410	0.561	0.9	0.290	0.979
HIST2H2AC	HIST1H2BL	9606.ENSP00000332194	9606.ENSP00000366618	0	0.000	0.000	0.410	0.561	0.9	0.290	0.979
CACNG2	LGI1	9606.ENSP00000300105	9606.ENSP00000360472	0	0.000	0.000	0.136	0.000	0.9	0.717	0.973
CACNG2	LGI1	9606.ENSP00000300105	9606.ENSP00000360472	0	0.000	0.000	0.136	0.000	0.9	0.717	0.973
FGA	APOA2	9606.ENSP00000306361	9606.ENSP00000356969	0	0.000	0.000	0.628	0.000	0.9	0.329	0.972
FGA	APOA2	9606.ENSP00000306361	9606.ENSP00000356969	0	0.000	0.000	0.628	0.000	0.9	0.329	0.972
CPA1	CELA3A	9606.ENSP00000011292	9606.ENSP00000290122	0	0.000	0.000	0.765	0.671	0.0	0.633	0.969
CPA1	CELA3A	9606.ENSP00000011292	9606.ENSP00000290122	0	0.000	0.000	0.765	0.671	0.0	0.633	0.969
FGA	SERPINA5	9606.ENSP00000306361	9606.ENSP00000333203	0	0.000	0.000	0.371	0.379	0.9	0.298	0.968
FGA	SERPINA5	9606.ENSP00000306361	9606.ENSP00000333203	0	0.000	0.000	0.371	0.379	0.9	0.298	0.968
CALCA	ADCYAP1	9606.ENSP00000331746	9606.ENSP00000462647	0	0.000	0.000	0.063	0.000	0.9	0.676	0.967
CALCA	ADCYAP1	9606.ENSP00000331746	9606.ENSP00000462647	0	0.000	0.000	0.063	0.000	0.9	0.676	0.967
CXCL13	CCL25	9606.ENSP00000286758	9606.ENSP00000375086	0	0.000	0.000	0.076	0.000	0.9	0.660	0.965
CXCL13	CCL25	9606.ENSP00000286758	9606.ENSP00000375086	0	0.000	0.000	0.076	0.000	0.9	0.660	0.965
MYL1	MYBPC1	9606.ENSP00000307280	9606.ENSP00000400908	0	0.000	0.000	0.596	0.000	0.9	0.215	0.965
MYL1	MYBPC1	9606.ENSP00000307280	9606.ENSP00000400908	0	0.000	0.000	0.596	0.000	0.9	0.215	0.965
HIST2H2AB	HIST1H2BL	9606.ENSP00000332790	9606.ENSP00000366618	0	0.000	0.000	0.455	0.368	0.9	0.128	0.965
HIST2H2AB	HIST1H2BL	9606.ENSP00000332790	9606.ENSP00000366618	0	0.000	0.000	0.455	0.368	0.9	0.128	0.965
HIST1H1D	HIST1H1E	9606.ENSP00000244534	9606.ENSP00000307705	0	0.000	0.000	0.651	0.000	0.9	0.862	0.964
HIST1H1D	HIST1H1E	9606.ENSP00000244534	9606.ENSP00000307705	0	0.000	0.000	0.651	0.000	0.9	0.862	0.964
CXCL13	CXCL5	9606.ENSP00000286758	9606.ENSP00000296027	0	0.000	0.000	0.000	0.000	0.9	0.654	0.964
CXCL13	CXCL5	9606.ENSP00000286758	9606.ENSP00000296027	0	0.000	0.000	0.000	0.000	0.9	0.654	0.964
APOA4	APOA2	9606.ENSP00000350425	9606.ENSP00000356969	0	0.000	0.000	0.115	0.000	0.9	0.626	0.964
APOA4	APOA2	9606.ENSP00000350425	9606.ENSP00000356969	0	0.000	0.000	0.115	0.000	0.9	0.626	0.964
AMBP	FGA	9606.ENSP00000265132	9606.ENSP00000306361	0	0.000	0.000	0.943	0.000	0.0	0.320	0.960
AMBP	FGA	9606.ENSP00000265132	9606.ENSP00000306361	0	0.000	0.000	0.943	0.000	0.0	0.320	0.960

PBF, PTTG1-binding factor.